

F/G 11/6

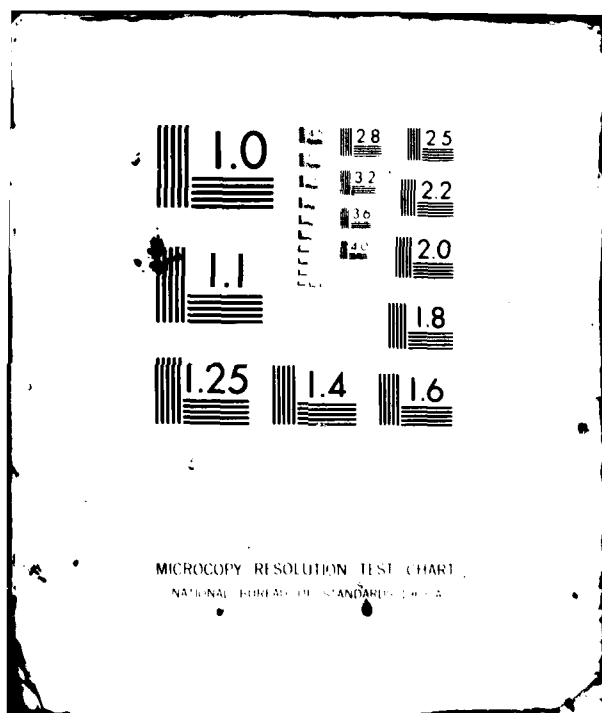
AFOSR-78-3732

AFOSR-TR-81-0882

NL.

$$\Delta_{\text{eff}} = \Delta_{\text{eff}}^{\text{eff}} + \Delta_{\text{eff}}^{\text{eff}}$$

END
DATE
FILMED
2 82
DTIC



UNCLASSIFIED

SECURITY CLASSIFICATION OF THIS PAGE (When Data Entered)

LEVEL II 12

AD A110217

REPORT DOCUMENTATION PAGE		READ INSTRUCTIONS BEFORE COMPLETING FORM
1. REPORT NUMBER AFCSR-TR- 31-0832	2. GOVT ACCESSION NO. AD-A110217	3. RECIPIENT'S CATALOG NUMBER
4. TITLE (and Subtitle) FATIGUE CRACK INITIATION AND PROPAGATION IN HIGH STRENGTH ALUMINUM P/M ALLOYS		5. TYPE OF REPORT & PERIOD COVERED Scientific-----Final 9/30/78 - 9/29/81
		6. PERFORMING ORG. REPORT NUMBER
7. AUTHOR(s) Morris E. Fine		8. CONTRACT OR GRANT NUMBER(s) AFOSR-78-3732
9. PERFORMING ORGANIZATION NAME AND ADDRESS Northwestern University Dept. of Materials Science & Engineering Evanston, Illinois 60201		10. PROGRAM ELEMENT, PROJECT, TASK AREA & WORK UNIT NUMBERS 2306/A1 61102F
11. CONTROLLING OFFICE NAME AND ADDRESS Air Force Office of Scientific Research Bolling AFB, Building 410 Washington, D. C. 20332		12. REPORT DATE November 30, 1981
		13. NUMBER OF PAGES 60 pages
14. MONITORING AGENCY NAME & ADDRESS (if different from Controlling Office) 12 62		15. SECURITY CLASS. (of this report) Unclassified
		15a. DECLASSIFICATION/DOWNGRADING SCHEDULE
16. DISTRIBUTION STATEMENT (of this Report) Approved for public release; distribution unlimited.		
17. DISTRIBUTION STATEMENT (of the abstract entered in Block 20, if different from Report) DTIC ELECTE JAN 29 1982 E		
18. SUPPLEMENTARY NOTES		
19. KEY WORDS (Continue on reverse side if necessary and identify by block number) Precipitation hardened aluminum powder metallurgy alloys Fatigue crack initiation Plastic work of fatigue crack propagation		
20. ABSTRACT (Continue on reverse side if necessary and identify by block number) Fatigue crack initiation in extruded X7091 RSP-P/M aluminum type alloys occurs at grain boundaries at low and at high stresses and thus the expected increase in crack initiation resistance from the smaller constituent particle size and grain size than in ingot alloys is not achieved. By a process of elimination the grain boundary embrittlement was attributed to Al_2O_3 particles formed during atomization and segregated to some grain boundaries. It is not due to the small grain size, to Co_2Al_3 , to η precipitates at grain boundaries nor to a precipitate free zone. Thermomechanical processing after extrusion of X7091 (done by Alcoa) with		

DD FORM 1 JAN 73 1473

UNCLASSIFIED

SECURITY CLASSIFICATION OF THIS PAGE (When Data Entered)

060720

DTIC FILE COPY

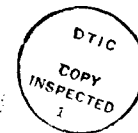
UNCLASSIFIED

SECURITY CLASSIFICATION OF THIS PAGE(When Data Entered)

Cu m Per Sq m

0.8% Co to produce large recrystallized grains resulted in initiation of fatigue cracks at slip bands and a much greater resistance to initiation of fatigue cracks at low stresses. Microcrack growth is faster in the thermomechanically treated samples as well as in ingot alloys than in the extruded and aged X7091. However, the threshold stress intensity range in the former is larger, 1.6 MN/m^2 compared to 0.9 MN/m^2 for extruded and heat treated samples. It would appear desirable to investigate fatigue crack initiation in much finer grained thermomechanically treated X7091-RSP-P/M alloys. These might have the higher resistance to fatigue crack initiation.

Accession For	
NTIS GRA&I	<input checked="checked" type="checkbox"/>
DTIC TAB	<input type="checkbox"/>
Unannounced	<input type="checkbox"/>
Justification	
By	
Distribution/	
Availability Codes	
Dist	Avail and/or Special
A	



UNCLASSIFIED

SECURITY CLASSIFICATION OF THIS PAGE(When Data Entered)

AFOSR-TR- 81 - 0882

LEVEL II

(12)

FINAL REPORT

on

FATIGUE CRACK INITIATION AND PROPAGATION IN HIGH
STRENGTH ALUMINUM P/M ALLOYS

covering period

30 September 1978 to 29 September 1981

by

Morris E. Fine

30 November 1981

DTIC
ELECT
JAN 29 1982
S E

This research was supported by Air Force Office of Scientific
Research, Air Force Systems Command USAF under Grant No. AFOSR-78-3732

DEPARTMENT OF MATERIALS SCIENCE AND ENGINEERING
THE TECHNOLOGICAL INSTITUTE ✓
NORTHWESTERN UNIVERSITY
EVANSTON, ILLINOIS 60201

82 01 29 002

Approved for public release; distribution unlimited

Approved for public release;
distribution unlimited.

INTRODUCTION

Outstanding monotonic mechanical properties and stress corrosion resistance have been achieved in powder metallurgy products made by forging or extruding hot pressed pre-alloyed rapidly solidified powder billets.¹⁻³ Particularly noteworthy is alloy X7091 (formerly designated by Alcoa as CT91 and MA87) which contains in wt.% 6.5 Zn, 2.5 Mg, 1.5 Cu, and 0.4 Co. In this alloy the dispersoid particles are Co_2Al_9 and Al_2O_3 . Because of the rapid solidification of the powders, these as well as any constituent particles are less than $0.5\text{ }\mu\text{m}$ in size. The designation RSP P/M in this report will mean a powder metallurgy processed alloy using rapidly solidified powders.

In a previous study of fatigue crack initiation in 2024-T4 aluminum alloy, it was shown that the probability for initiating a fatigue crack at constituent particles dropped rapidly as the inclusion size normal to the stress direction decreased below $6\text{ }\mu\text{m}$. This probability was quite small for $2\text{ }\mu\text{m}$ sized inclusions, the smallest size measured. Below this size it was difficult to distinguish constituent particles from dispersoids added for grain refinement. The initiation mode was along slip bands which emanated from the inclusions.

Further, in the previous study⁴ 2124, a high purity version of 2024 prepared by Alcoa, was included. The volume of constituent particles in the 2124 was less than 1/10 that in 2024. This was achieved in part by using a high temperature solution treatment to eliminate S-phase but a large grain size resulted. Slip band fatigue cracks unassisted by inclusions formed more easily in the coarse grained 2124 than in the finer grained 2024. In RSP P/M 7091, since the grain size as well as the constituent and

dispersoid particles are much smaller than in 2024, a greater resistance to fatigue crack initiation is expected than in conventional ingot precipitation hardened alloys. Earlier studies of the fatigue life of some RSP-P/M aluminum alloys indicated them to be better than some ingot alloys.⁵ This seemed likely to be due to improved fatigue crack initiation resistance. For these reasons studies of fatigue crack initiation, microcrack growth, and near-threshold stress intensity range (ΔK_{th}) growth of macrofatigue cracks were undertaken. Concurrent with the present research, Lawley and Koczak undertook, also under AFOSR sponsorship, a study of fatigue in similar alloys.⁶ Their research concentrated on fatigue life and crack propagation rates at intermediate levels of stress intensity range. In addition, Starke⁷ is presently studying the effects of microstructural modification through various thermomechanical treatments on fatigue properties.

The present report is divided into three parts:

- I. Fatigue crack initiation
- II. Fatigue microcrack propagation
- III. Near threshold growth of fatigue macrocracks

I. Fatigue crack initiation in RSP-P/M 7091 type alloys

A. Experimental Details

A series of alloys of varying Co content prepared by Alcoa Research Center² for an Air Force Materials Lab sponsored research program was made available for the present research. The compositions of the alloys and their fabrication and heat treatments are shown in Table I. The grain sizes are also shown in Table I. These decreased slightly with increase


Accession For	
NTIS GRA&I	<input checked="checked" type="checkbox"/>
DTIC TAB	<input type="checkbox"/>
Unannounced	<input type="checkbox"/>
Justification	
By	
Distribution/	
Availability Codes	
Dist	Avail and/or Special
	

TABLE I.

ALLOY COMPOSITIONS, FABRICATION, AND HEAT TREATMENTS

a) Chemical Composition (from Alcoa)

<u>Alloy</u>	<u>Zn</u>	<u>Mg</u>	<u>Cu</u>	<u>Co</u>
0 Co	6.28	2.44	1.47	0.0
0.4 Co(X7091)	6.46	2.42	1.49	0.38
0.8 Co	6.60	2.54	1.53	0.85

Compositions are in wt.%

Extrusion strain rate: 2.6×10^{10} /sec, to plates
1.27 cm thick x 16.5 cm wide³

b) Heat Treatment of 0-0.8 Co Alloys

- Solution treated, 2 hrs at 488°C
- Aged 5 days at R.T., stretched 3% to reduce residual stress
- Aged 24 hrs at 121°C (peak aged)
- Aged 4 hrs at 163°C (overaged)
- Average grain size $7 \mu\text{m} \times 3.5 \mu\text{m} \times 2 \mu\text{m}$

c) Thermo Mechanical Treatment (TMT) of 0.8 Co Alloy

- Annealed, 2 hrs at 413°C - cooled to 204°C
Reheated 4 hrs at 232°C - cooled to R.T.
- Cold-rolled 50% at R.T. to 0.25 in.
- Solution treated 2 hrs at 471°C + 2 hrs at 488°C
- Quenched in water at 49°C, stretched 1.5-2.0%
- Aged 4-5 days at R.T.
- Aged 24 hrs at 121°C (peak aged)
- Aged 4 hrs at 163°C (overaged)
- Average grain size $115 \mu\text{m} \times 93 \mu\text{m} \times 38 \mu\text{m}$

Done by Robert Sanders, Jr. at Alcoa Research Lab

in Co content. The 1.27 cm thick plates were received in the peak aged condition. The overaging treatment was done at Northwestern.

Most of the tests were done on panel specimens $100 \times 10 \times 3.5$ mm containing notches introduced with milling cutters. The notch base was polished in the stress direction to a finish of $1 \mu\text{m}$ and slightly etched to reveal grain boundaries, although some tests were on unetched specimens. The majority of the tests were done on specimens with U-shaped notches 1.70 ± 0.03 mm deep with a notch radius of 0.65 ± 0.02 mm. Some tests were also done with specimens containing U-shaped notches 2mm deep and 25.4 mm radius of curvature, semi-circular notches of 0.6 and 0.99 mm radii, and with unnotched specimens of 4 mm gage length similarly polished and lightly etched.

All of the tests were done with an MTS electrohydraulic servo-valve controlled testing machine of 90 KN capacity in laboratory air of 30-40% relative humidity. As previously, an Olympus long working distance 800X magnification metallurgical microscope with camera attachment was mounted directly on the testing machine for visual observation during cycling.⁴ Replicas of the unnotched and blunt notched specimen surfaces were also taken for electron microscope study.

Cyclic and monotonic yield stress values (0.2% offset) of the P/M alloys are given in Table II for the longitudinal (L) and long transverse (LT) directions, as determined by the incremental step technique. The longitudinal direction is the extrusion direction. The monotonic results are in reasonable agreement with those reported previously.³ In the extruded and heat treated specimens there is little effect of Co content. While there is little difference between σ_y and σ_y' for the L direction,

TABLE II.
MONOTONIC AND CYCLIC YIELD STRESS

	σ_y	σ_y'	σ_y	σ_y'
	L		LT	
RSP-P/M 0.0% Co OA	545	554	566	523
RSP-P/M 0.4% Co (X7091) OA	553	540	555	528
RSP-P/M 0.8% Co OA	550	555	565	538
RSP-P/M 0.8% Co TMT PA	555	558	-	-
RSP-P/M 0.8% Co TMT OA	504	530	-	-

Units: MN/m^2 , values are averages of two measurements
 σ_y : 0.2% monotonic yield stress; σ_y' : 0.2% cyclic yield stress

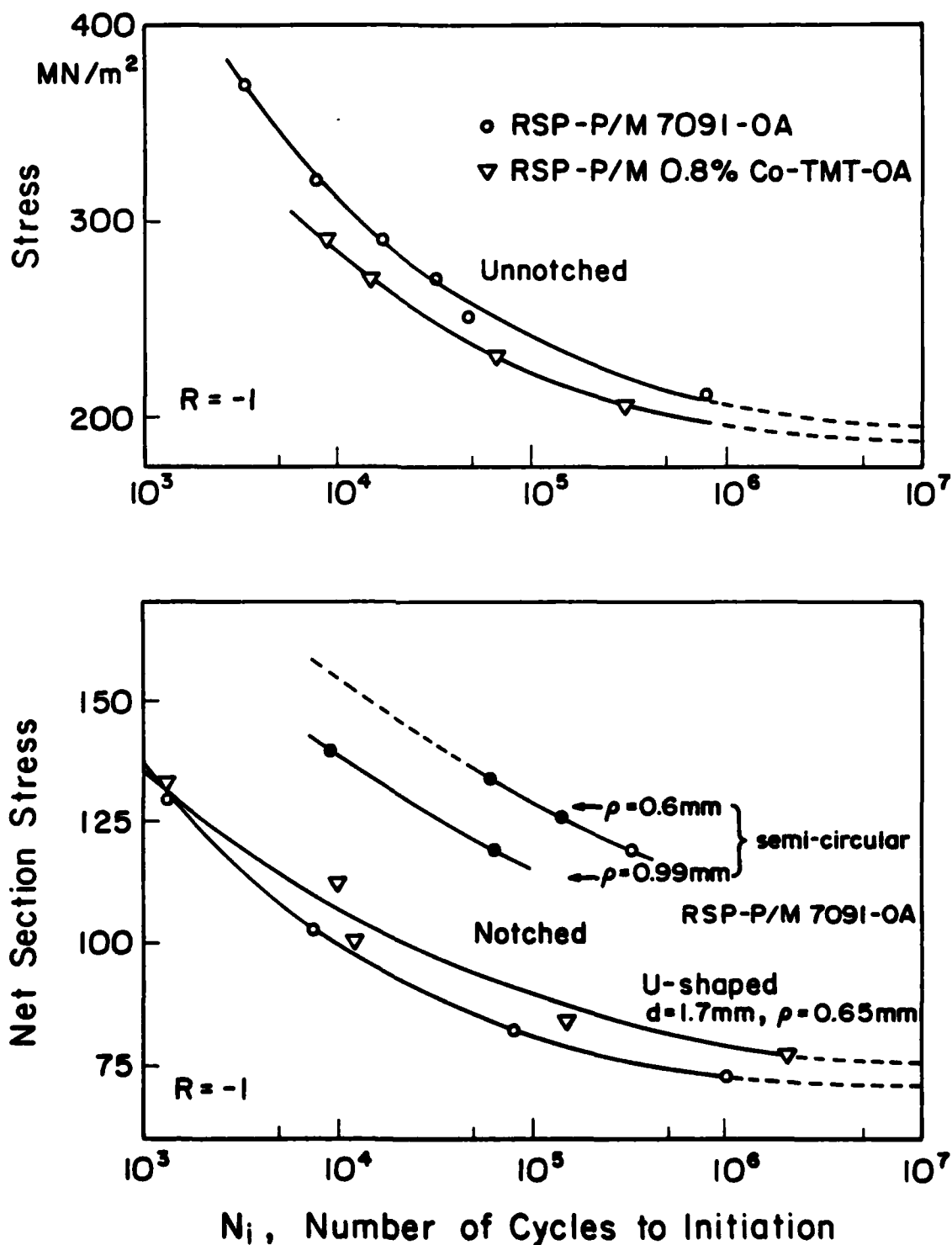
the LT direction shows cyclic softening. After the thermomechanical processing, precipitation hardening to peak strength (PA) gives approximately the same strength as extruded and overaged samples. Overaging reduces σ_y but cyclic hardening is observed for this treatment.

In order to ascertain the actual stresses at the bases of the various notches, notched and unnotched specimens were cycled with $R = -1$ to crack initiation (N_i is the cycles to crack initiation). Then $K_{fi}(N_i(\text{unnotched})/N_i(\text{notched}))$ was compared with K_t , the stress concentration factor calculated from elasticity theory. As will be discussed thoroughly in this paper, in the as-extruded and heat treated samples the fatigue cracks initiated along grain boundaries; N_i was defined as initiation of a 10 to 20 μm grain boundary crack. This was done for RSP-P/M X7091 as extruded-overaged and RSP-P/M 0.8% Co-TMT and overaged. The results are given in Fig. 1 where for the notched sample the net section stress is plotted. The resulting values of K_{fi} are plotted in Fig. 2. The K_{fi} values decrease with decrease in load, i.e., cycles to crack initiation. The thermomechanical processed 0.8% Co samples have lower values of K_{fi} .

The elastic stress concentration factor, K_t , determined from charts published by Peterson⁸ based on Neuber's⁹ treatment is 2.64. This is indicated by arrows on the right and lefthand sides of Fig. 2. One expects K_{fi} to approach K_t as the stress is reduced and the behavior becomes more nearly elastic. This appears to hold for the extruded and overaged RSP-P/M X7091 but not for the TM processed 0.8% Co samples where K_{fi} for low stress-high N_i is 15% lower than K_t .

Since K_t is better known for semi-circular notched samples,

Fig. 1. Number of cycles to fatigue crack initiation, N_i , versus maximum stress (stress amplitude). The upper figure is for unnotched specimens and the lower for notched specimens of notch dimensions indicated on the figure. In the lower figure the maximum nominal net section stress at the notch is plotted. N_i is defined as a 10-20 μm grain boundary crack for RSP-P/M 7091-OA and a 10-20 μm slip band crack for RSP-P/M 0.8% Co-TMT-OA.



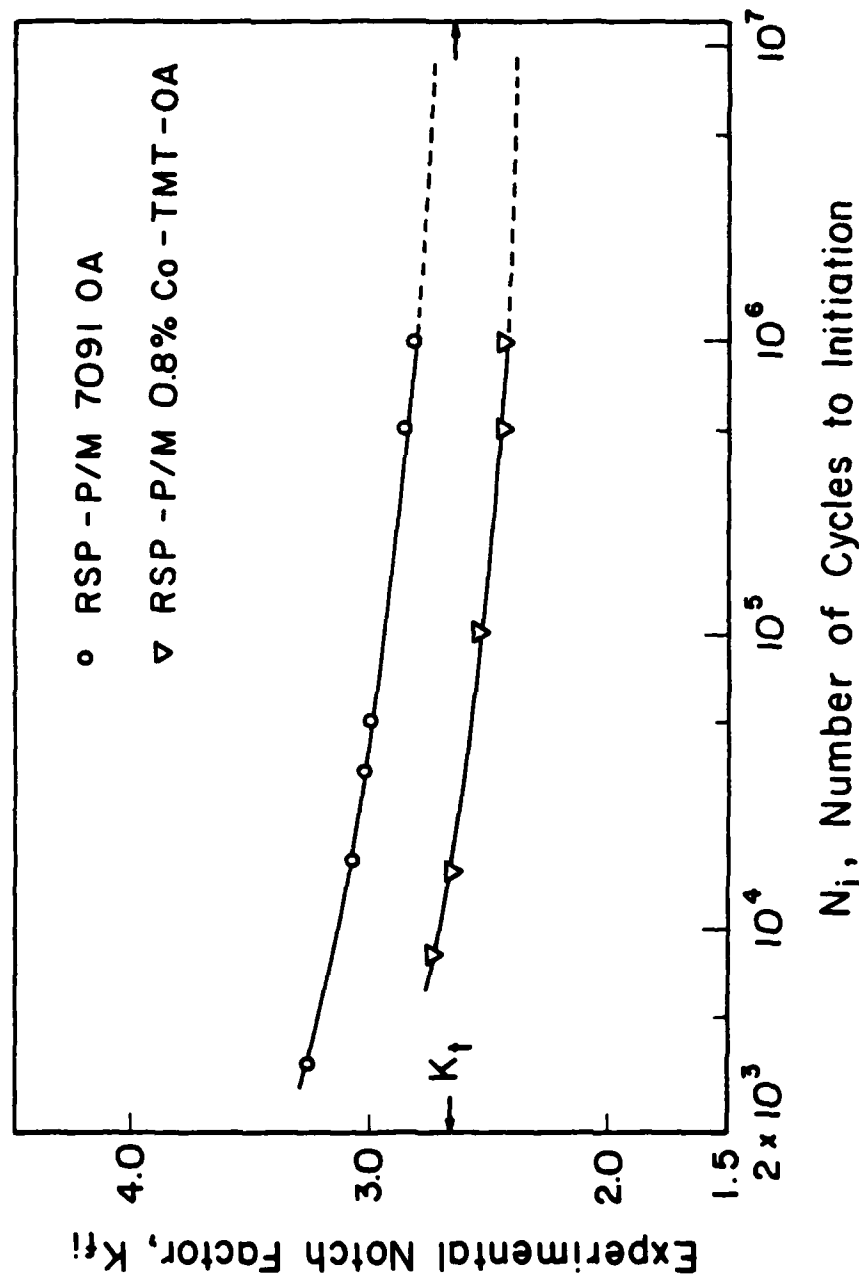


Fig. 2. Experimentally determined stress concentration factor, K_{fi} , versus N_i where K_{fi} is the ratio of N_i (unnotched) to N_i (notched) and the N_i 's are from Fig. 1. The arrows indicate the elastic stress concentration factor for the notch geometry determined from the charts in Peterson's book.⁸

several semi-circular notched samples of RSP-P/M X7091-OA were also tested. These results are also shown in Fig. 1 and K_{fi} and K_t are compared in Fig. 3. It appears that K_{fi} at high values of N_i is generally lower than K_t . Unfortunately, we were unable to find similar data in the literature comparing microscopic fatigue crack initiation for notched and smooth specimens to determine K_{fi} . Thus the generality of the present results has not been established.

For the present study where a U-shaped notch 1.7 mm deep and 0.65 mm radius of curvature was mainly used, the stress concentration factor was taken to be K_t or 2.64, the value determined from Peterson's graphs.

B. Results and Discussion

1. Fatigue crack initiation in extruded and heat treated alloys

The first series of fatigue crack initiation studies were fully reversed ($R = -1$) stress controlled tests of samples of the RSP-P/M 0.0% Co, 0.4% Co (X7091), 0.8% Co alloys which were overaged after extrusion and solution treatment as described in Table I(b). This aging treatment was selected because it is the preferred one due to its stress corrosion cracking resistance. In all three alloys so processed at all stress levels whether high or low, the first indication of a fatigue crack was "widening" of a grain boundary segment when the load was near the maximum tensile load. When the load was compressive or zero these "wide" grain boundaries initially had normal widths, but later the grain boundary cracks were open at all stress levels. The initial grain boundary cracks grew into adjacent grain boundaries and additional cracks initiated as the cycling continued. Grain boundary fatigue cracks formed whether the notch surfaces were etched or not.

Starke and Walker¹⁰ also observed fatigue crack initiation along grain boundaries in strain controlled tests of RSP-P/M X7091 at all total strain

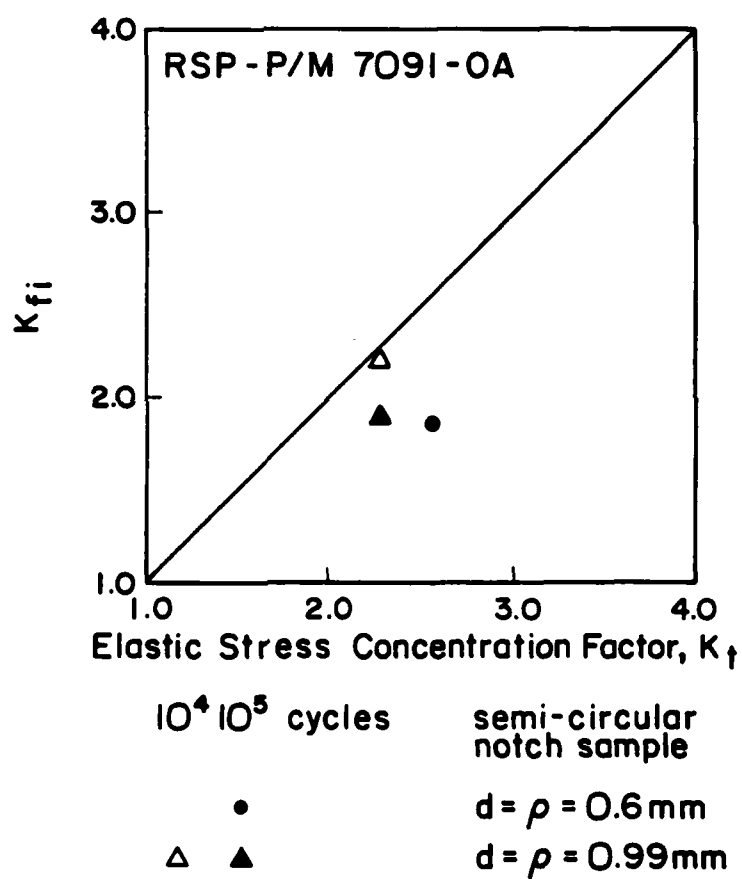


Fig. 3. Comparison of K_{fi} and K_t for semicircular notches in RSP-P/M 7091-OA of two different radii of curvature for N_f 's of 10^4 and 10^5 cycles.

amplitudes studied, 0.0085 to 0.02. Observations of thin foils of samples cycled to failure at 0.002 plastic strain amplitude using TEM revealed occasional persistent slip bands within regions of high dislocation density; however, extensive SEM studies of the specimens' surfaces revealed no coarse slip traces.

Figure 4 shows the same region of the notch surface before cycling and after 1500 cycles at a nominal (net-section) stress of 136 MN/m^2 . The photo micrograph was taken at zero applied stress. Such cracks were first noted after 500 cycles but did not remain open at zero stress as already discussed.

The arrows denoted A and B in Fig. 4 are the same dark region on the notch surface. It, as well as other smaller dark regions, are probably pits introduced during notch preparation. The large dark region (A and B) probably is due to the initial presence of a large inclusion. Their effect on fatigue will be discussed later.

Grain boundary fatigue cracks in a specimen cycled 415,000 cycles at a nominal net section stress of 77 MN/m^2 are shown in Fig. 5. Two different areas (a and b) of the notch area are shown. At this stress, the first grain boundary crack was noted after 15,000 cycles. In general, the number of grain boundary crack initiation sites decreased as the nominal stress was decreased.

It is often assumed that fatigue crack initiation represents 90% of the lifetime in the high cycle regime. This is not true for the present alloys. This also will be discussed later, in section II.

Defining N_{ii} as the number of cycles to the first indication of a grain boundary crack, as observed by the microscope attached to the apparatus, this quantity was measured over a wide range of nominal stress values

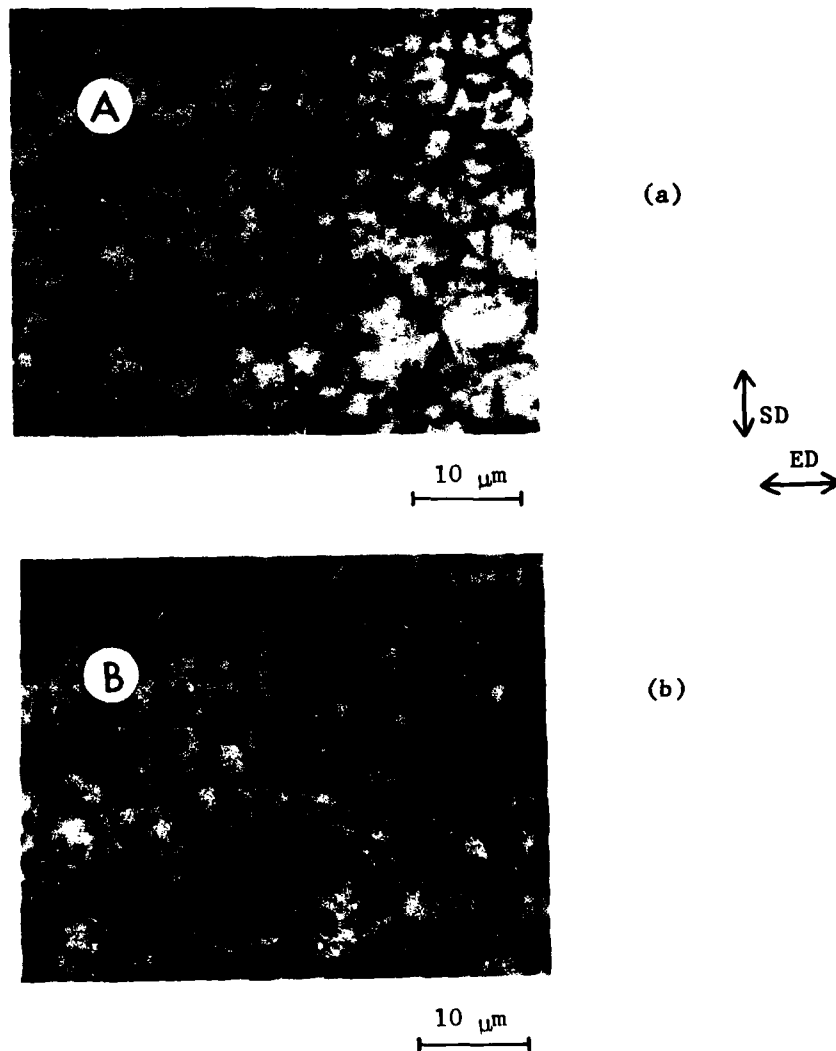
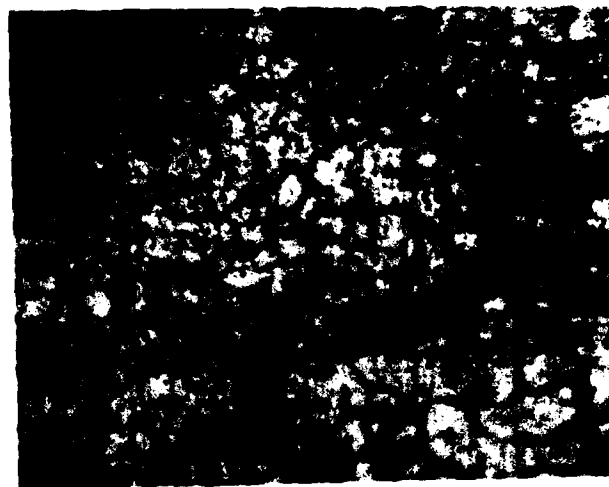
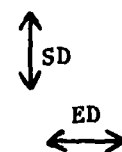


Fig. 4. Optical micrographs of same area of notch surface of specimen of RSP-P/M 0.8%-OA which was cycled 0 (a) and 1500 (b) cycles at a maximum nominal net section stress of 136 MN/m^2 with R of -1 . The notch-specimen orientation was L_n (see Fig. 8). The notch geometry ($K_t = 2.64$) is shown in Fig. 8. SD is the stress direction and ED is the extrusion direction. A and B denote the same defect. N_{11} was 500 cycles.



(a)

20 μm



(b)

20 μm

Fig. 5. Optical micrographs of notch surface ($L_n, K_t = 2.64$) of RSP-P/M 7091-OA after 415,000 cycles ($R = -1$) at a nominal maximum net section stress of 77 MN/m^2 . N_{ii} was 15,000 cycles.

in all three alloys, extruded, solution treated and overaged. The results are plotted in Fig. 6. Here N_{ii} , plotted along the horizontal axis, corresponds to a 5 to 10 μm crack along a grain boundary segment while the vertical axis is $\log K_t \sigma_{\text{max}}$. The stress range is twice σ_{max} so the nominal stress range may be obtained by dividing the numbers plotted by 1.32.

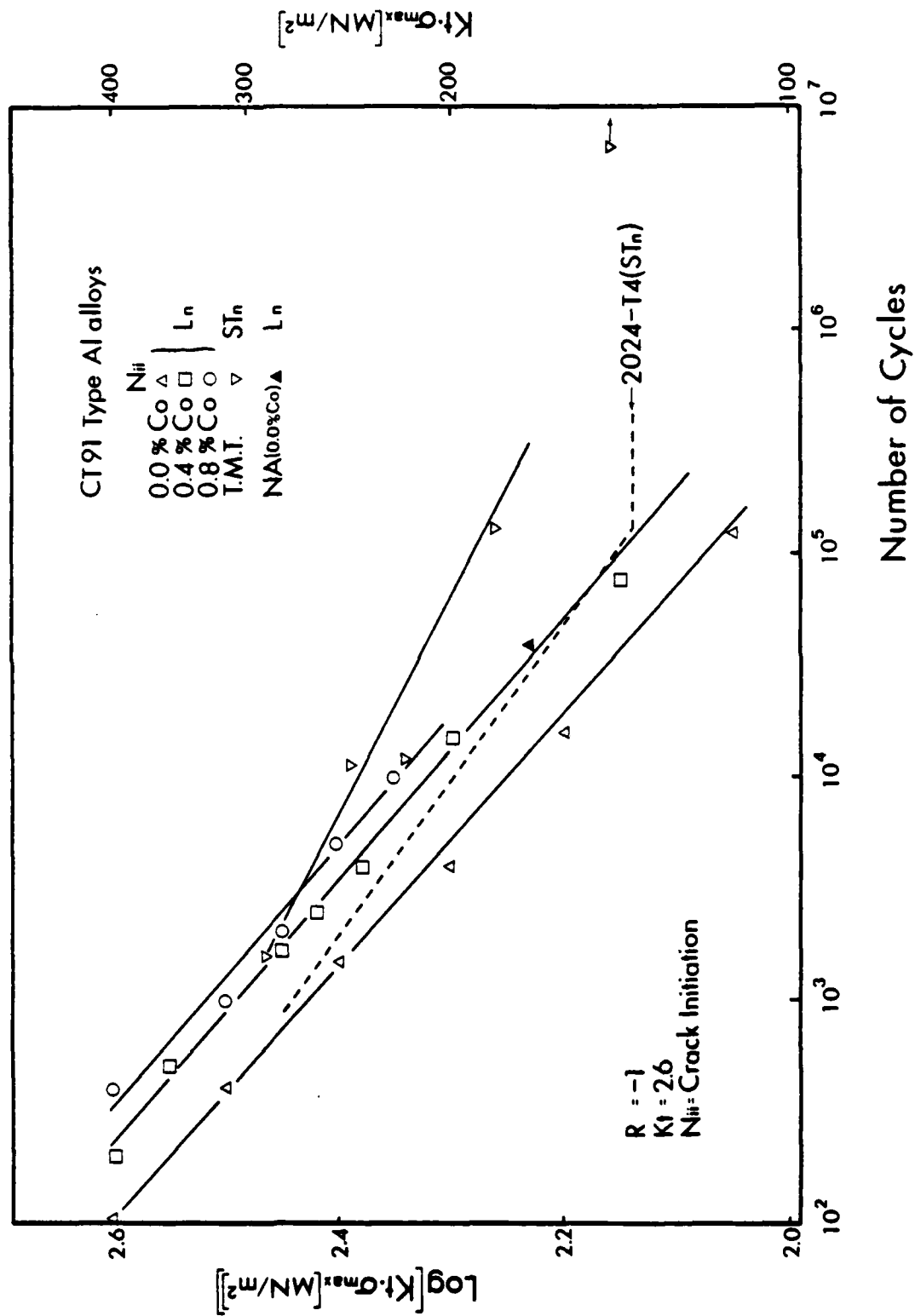
Figure 6 also shows data for thermomechanically treated samples and samples aged only at room temperature. These will be considered later.

The data for $\log N_{ii}$ vs. $\log \sigma_{\text{max}}$ follows a linear relation out to 10^5 cycles. The lines for the three Co contents are parallel but displaced to longer N_{ii} 's as the Co content is increased. The previous data⁴ for 2024-T4 is plotted for comparison and the $\log N_{ii}$ vs. $\log \sigma_{\text{max}}$ line is seen to lie in the range of the lines for RSP-P/M X7091 type alloys. Of course, for 2024-T4 the fatigue cracks initiated along slip bands. The expected increase in N_{ii} for the RSP-P/M alloys was not achieved presumably because of the grain boundary embrittlement.

Since the grain boundary fatigue crack initiation might possibly be a function of grain orientation due to anisotropy introduced by the extrusion, specimens of three orientations were investigated as shown in Fig. 7. The data discussed so far were for the Ln orientation. Specimens oriented LTn and STn also initiated fatigue cracks along grain boundaries. Figure 8 compares N_{ii} versus nominal maximum net section stress for RSP-P/M X7091-OA for the STn and Ln specimen orientations. The N_{ii} values for the STn notch-specimen orientation are very slightly higher.

No evidence for slip bands were noted on the notch surface even at high stresses using either optical or scanning electron micrographs. Thus the slip steps must be very small. Figure 9 shows a scanning electron

Fig. 6. Number of cycles to initiation of 5 μm cracks in extruded and heat treated X7091 type alloys (CT91) versus $K_t \sigma_{\text{max}}$. The notch geometry and orientations are shown in Fig. 7. Data for 2024-T4 is shown for comparison. $K_t = 2.64$. σ_{max} is the maximum nominal net section stress. The nominal stress range, $\Delta\sigma$, is $2\sigma_{\text{max}}$. Except for NA (naturally aged) and TMT data, the samples were extruded, solution treated and overaged. After TMT, the samples were solution treated and peak aged (Table I-c).



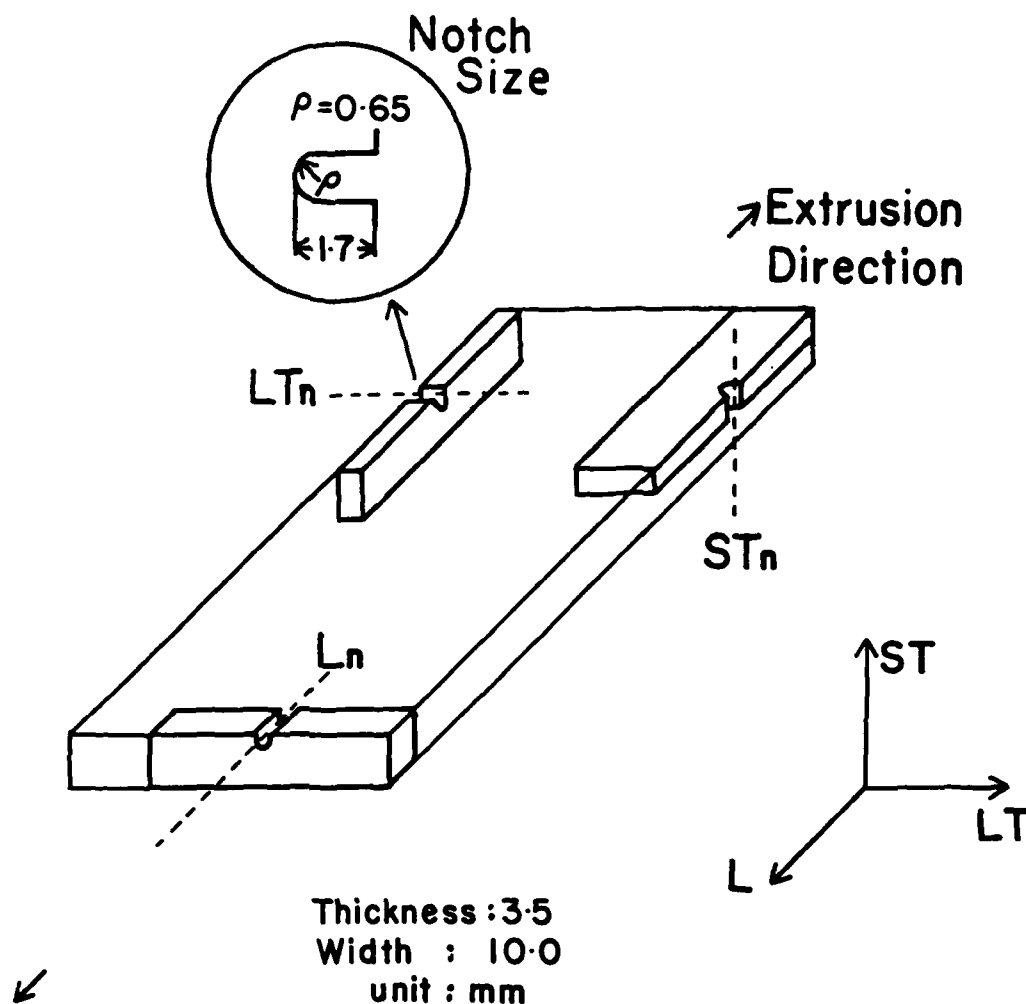


Fig. 7. Orientation of specimens and notches with respect to the extrusion direction. For 2024 this is the rolling direction. The specimen dimensions and notch dimensions are also shown.

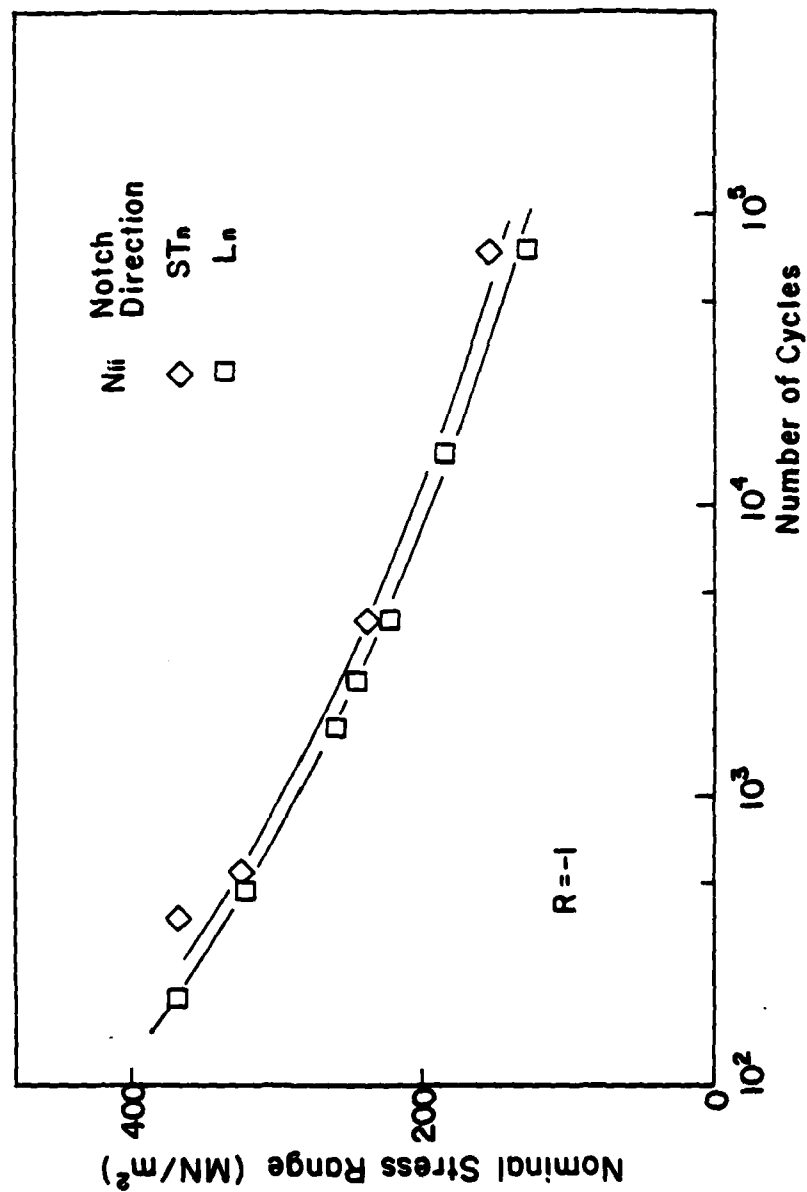


Fig. 8. N_{11} of RSP-P/M 7091-OA vs. $K_t \sigma_{max}$ for STn and Ln orientations. The notch size and geometry are shown in Fig. 7. $K_t = 2.64$.

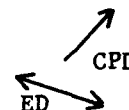
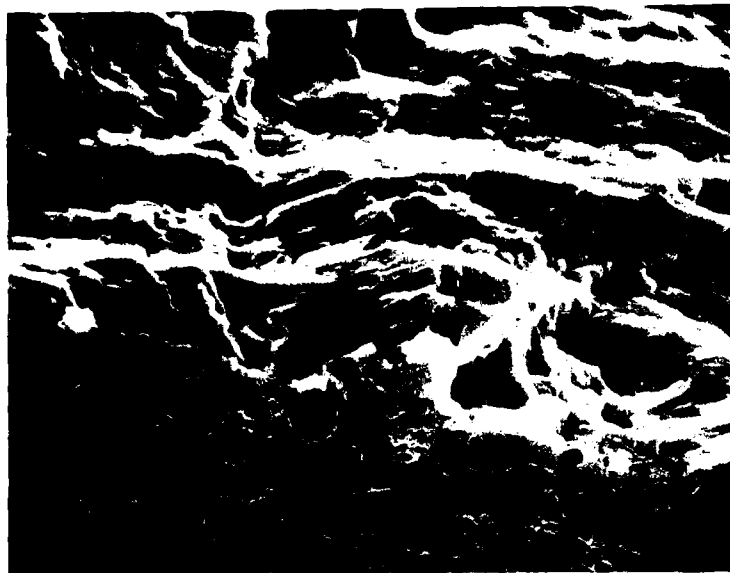


Fig. 9. Scanning electron micrograph of notch surface and fracture surface of RSP-P/M 0.8% Co-OA after cycling at a nominal maximum net section stress of 97 MN/m^2 . The specimen was broken statically. The static fracture is out of the field of view. Standard $K_t = 2.64$ notch, $R = 0.1$. Notch orientation was Ln. CPD is crack propagation direction. Magnification 1900 times.

micrograph of the notch and fracture surface after fatiguing 6000 cycles at a maximum nominal stress of 193 MN/m^2 . The specimen was pulled to failure in tension to facilitate SEM observation. The monotonic fracture surface is outside the field of the figure. The R-ratio was 0.1 to avoid damaging the fracture surface. The fracture surface is observed to intersect the notch surface mainly at grain boundaries. No evidence of slip lines on the notch surface are seen.

In order to investigate further for evidences of plastic deformation associated with the grain boundary fatigue crack initiation, a specimen of RSP-P/M 0.0% Co-OA with a blunt notch (2 mm deep and 25.4 mm radius of curvature, $K_t = 1.25^8$) was cycled to N_{ii} (510 cycles) at a nominal maximum net section stress of 168 MN/m^2 and then a replica for TEM was taken. The blunt notch rather than the standard notch was used to facilitate surface replication. The resulting TEM micrograph of the replica of the fatigue crack initiation site at 10,000 times magnification is shown in Fig. 10. There is no clear evidence of slip line formation; however, two shallow lines are seen to radiate from the crack which may possibly be slip lines.

For purposes of discussing the origin of the grain boundary embrittlement, a transmission electron micrograph of a thin foil of RSP-P/M X7091-OA is shown in Fig. 11. The structure shown is essentially identical to those already published.^{2,3} The Co_2Al_9 particles may be eliminated as the cause of the embrittlement because they are not segregated to grain boundaries. Further, grain boundary fatigue cracks formed in the 0.0% Co samples.

Overaging gives a precipitate free zone and η particles at grain boundaries which must be considered as a source of the embrittlement. During aging at 121°C to peak strength very small precipitates concentrate

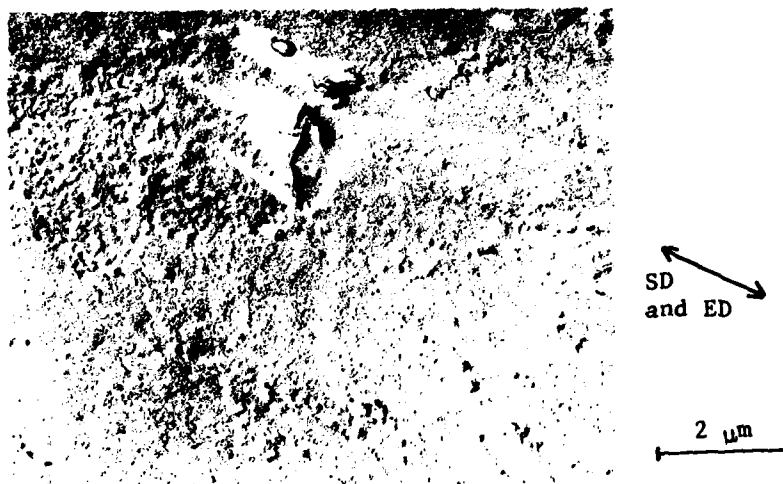


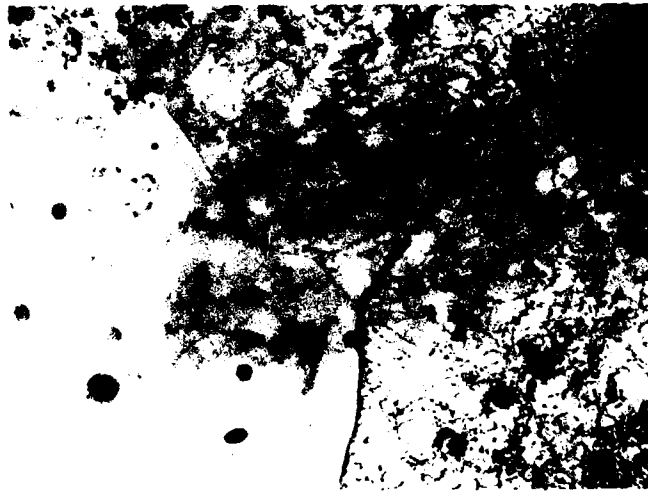
Fig. 10. Transmission electron micrograph of single stage replica of specimen of RSP-P/M 0.0% Co-OA with blunt (2 mm deep, 25.4 mm radius of curvature) notch of $K_t = 1.25$ cycled to N_{ii} (510 cycles) at a nominal maximum net section stress of 168 MN/m^2 . Replica was shadowed with Au-Pd and then coated with carbon. Notch-specimen orientation was STn.



Fig. 11. Transmission electron micrograph of thin foil of RSP-P/M 7091-OA. A precipitate free zone and η particles are seen at grain boundaries. The large dark particles are Co_2Al_9 . The white patched regions are where Co_2Al_9 was removed during thinning.

near grain boundaries but there is no evidence of a precipitate free zone as shown in Fig. 12. A specimen of RSP-P/M X7091 with a standard $K_t = 2.64$ notch was aged 24 hrs at 121°C and tested at a maximum net section stress of 76.7 MN/m^2 ($R = -1$). The fatigue cracks also initiated at grain boundaries. It was, therefore, decided to study specimens which were naturally aged (NA) i.e., only aged at room temperature. Specimens of the RSP-P/M X7091 type alloys which had been previously peak aged (as-received condition) were resolution treated for 2 hrs at 488° , water quenched, and aged at room temperature. During the room temperature age they were stretched 3%. The resulting grain size was larger after the treatment being $100 \mu\text{m}$ in the extrusion direction and $15 \mu\text{m}$ in the long transverse direction. However, subgrains not visible under the light etching must have been present because they were seen after cycling and were clearly seen after aging at 121°C . Presumably η' decoration of subgrain boundaries had occurred. As shown in Fig. 13 the grain boundaries after room temperature aging appear clean and show no evidence for a grain boundary precipitate.

A standard notch sample ($K_t = 2.64$) of the naturally aged 0.0% Co alloy was cycled at a maximum nominal net section stress of 75 MN/m^2 ($R = -1$) and carefully examined with the 800 times magnification microscope attached to the MTS machine. The larger grain size facilitated optical observation. After 20,000 cycles small pits appeared inside the grains. They were observed in the grain boundaries after 25,000 cycles. The damage increased with cycling particularly at the junction of grain boundaries. After 40,000 cycles what appeared to be a definite crack less than $5 \mu\text{m}$ long appeared at a grain boundary junction. This was taken to be N_{ii} and the point is plotted in Fig. 6. The number of pits inside the grains increased



1 μm

Fig. 12. TEM micrograph of thin foil RSP-P/M 7091-PA. After peak aging very small precipitates are seen at grain boundaries but there is no precipitate free zone.



(a)



(b)

1 μm

Fig. 13. TEM micrographs of thin foils of RSP-P/M 0.8% Co naturally aged (NA). Previously peak aged alloy was resolution treated 2 hrs at 488°C, cold water quenched and aged 7 days at room temperature. During the aging it was stretched 3%. The grain boundaries in (a) show no evidence of a grain boundary precipitate nor a precipitate zone; however, in (b) there are particles at grain boundaries which are believed to be aluminum oxide.

with cycling as well as in the grain boundaries and outlined subgrains about 10 μm in diameter. After 160,000 cycles the largest crack was 30 μm long. It occurred in a grain boundary and ran between two subgrain boundary-grain boundary intersections. The pits may have formed by popping out of dispersed intermetallic particles or oxides, as suggested by Walker and Starke.¹⁰ The fatigue cracks initiated along grain boundaries in the room temperature aged samples of the RSP-P/M 0.8% Co and X7091 alloys as well, except in samples with blunt notches transgranular cracks were seen near inclusions. This will be discussed later.

Since the room temperature aged specimens had neither η precipitates nor a precipitate free zone at the grain boundaries, none of these can be responsible for the grain boundary embrittlement.

2. Fatigue crack initiation in thermomechanically processed RSP-P/M 0.8% Co alloy

It was next considered that the presence of oxide particles at some grain boundaries originating from the atomization might be responsible for the initiation of fatigue cracks at grain boundaries. It is well-known that such oxide particles are present and pin the grain boundaries.^{2,3} It was considered that further mechanical processing and annealing might result in a structure where the grain boundaries are free of oxide particles and thus might increase the resistance to fatigue crack initiation. In order to test this hypotheses, Dr. R. Sanders, Jr. of Alcoa Technical Center made available to us the thermomechanically processed material described in Table I(c). The monotonic and cyclic yield stresses for the longitudinal stress direction (extrusion direction) are shown in Table II for samples aged to peak strength and overaged. As already noted, the

strength of the peak aged TMT 0.8% Co alloy is approximately the same as overaged for extruded and heat treated. While the monotonic yield stress of the overaged TMT 0.8% Co alloy is 10% lower, it cyclically hardens so the reduction in cyclic yield stress is much smaller. The thermomechanical treatment detailed in Table I(c) resulted in a much larger grain size which is no doubt responsible for the reduction in strength. As noted in Table I(c), the average grain size was 115 μm by 93 μm by 38 μm . Figure 14 shows the grain structure of the TMT-0.8% Co alloy. There are many steps in the grain boundaries and these increase the fatigue life.¹¹

The TMT 0.8% Co alloy received from Alcoa was aged 24 hrs at 121°C (PA) which does not result in grain boundary precipitate free zones. Some of the samples were additionally aged 4 hrs at 163°C to give PFZ and larger η in the grain boundaries (OA). The fatigue crack initiation mode in samples of both TMT-PA and TMT-OA is transgranular and not intergranular as in extruded and heat treated RSP-P/M 7091 type alloys. Figure 15 shows microcracks along slip lines in PA and OA samples. Small slip bands parallel to the crack are also observed. When the microcrack intersects a grain boundary, a change in the direction of the crack occurs no doubt because slip is discontinuous across grain boundaries. The fatigue cracks sometimes appeared to originate from pits which were produced by the stress cycling. Such a fatigue microcrack is shown in Fig. 16. The pit shown is approximately 2 μm in diameter. Many such pits probably originate from popping out of intermetallic or oxide dispersoid particles.

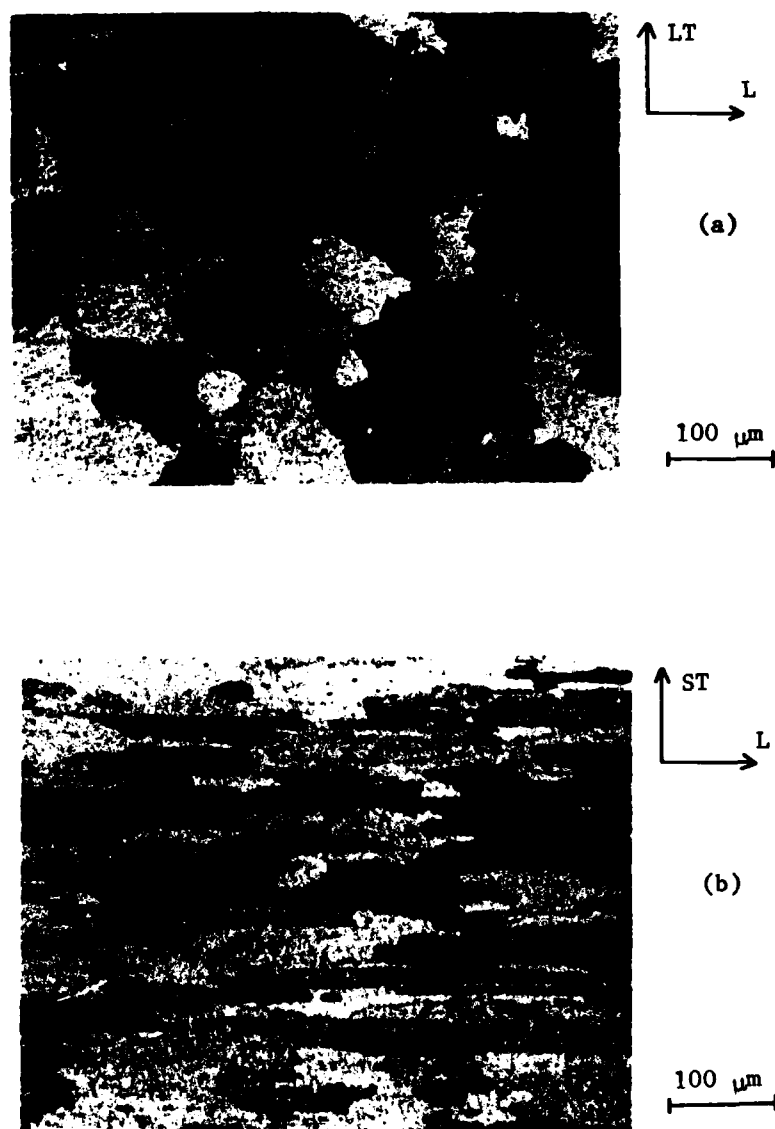


Fig. 14. Optical micrographs showing grain structure of RSP-P/M 0.8% Co-TMT-OA. (a) Surface normal to short transverse (ST) direction. (b) Surface normal to long transverse (LT) direction. L is longitudinal direction.



Fig. 15. Optical micrographs showing fatigue microcracks in RSP-P/M 0.8% Co-TMT samples containing standard $K_t = 2.64$ notches. STn specimen and notch orientation.

- (a) Peak aged. Sample was cycled 1500 times at a maximum nominal net section stress of 111 MN/m^2 with $R = -1$. N_{11} was 1400 cycles. Note microcrack is along a slip band. Other slip bands are indicated by the arrows.



Fig. 15. (b) Overaged. Sample was cycled 7000 times at a maximum nominal net section stress of 100 MN/m^2 with $R = -1$. N_{11} was 6000 cycles. Note slip line crack changes direction at grain boundaries.



Fig. 16. Optical micrograph of fatigue crack in RSP-P/M 0.8% Co-TMT-OA which appears to have originated at a pit. Standard $K_t = 2.64$ notch. Maximum nominal net section stress was 90 MN/m^2 with $R = -1$. N of figure is 11,000 cycles. N_{ii} was 9000 cycles. Pit appeared during stress cycling and is probably due to popping out of an inclusion.

The cycles to fatigue crack initiation, N_{ii} , for the peak aged TMT 0.8% Co alloy samples are compared to N_{ii} for the extruded and overaged 0.8% Co alloy in Fig. 6. At low stresses, the thermomechanical treatment clearly gives greater resistance to fatigue crack initiation by a considerable amount. The results for the TMT peak aged and overaged give nearly identical results, as shown in Fig. 17. Thus removing the origin of the grain boundary cracking by TMT is highly beneficial to fatigue crack initiation. We propose the TMT-recrystallization treatment produces grain boundaries containing relatively few oxide particles so that the alloy is not subject to initiation of fatigue cracks at grain boundaries.

While the thermomechanical treatment detailed in Table I(c) results in grain growth, Starke and co-workers¹² have done additional research on thermomechanical processing to yield smaller grain sizes. The small grain sized TMT samples have increased strain controlled fatigue lifetimes. It would be desirable to study fatigue crack initiation by the present methods in these smaller grained thermomechanically processed RSP-P/M X7091 type alloys.

3. Role of inclusions on initiation of fatigue cracks

An occasional large inclusion was noted in the RSP-P/M X7091 type alloys utilized in this investigation. These are sites of fatigue crack initiation in these alloys as in conventional alloys. The probability for the occurrence of such inclusions in the notch section increases as the notch width and radius of curvature were increased. Thus while fatigue crack initiation at inclusion sites was seldom seen with $K_t = 2.64$ notches, it was more frequently seen with the $K_t = 1.25$ notches. Figure 18a and b show a large pit in an RSP-P/M X7091-OA sample before and after 19,000

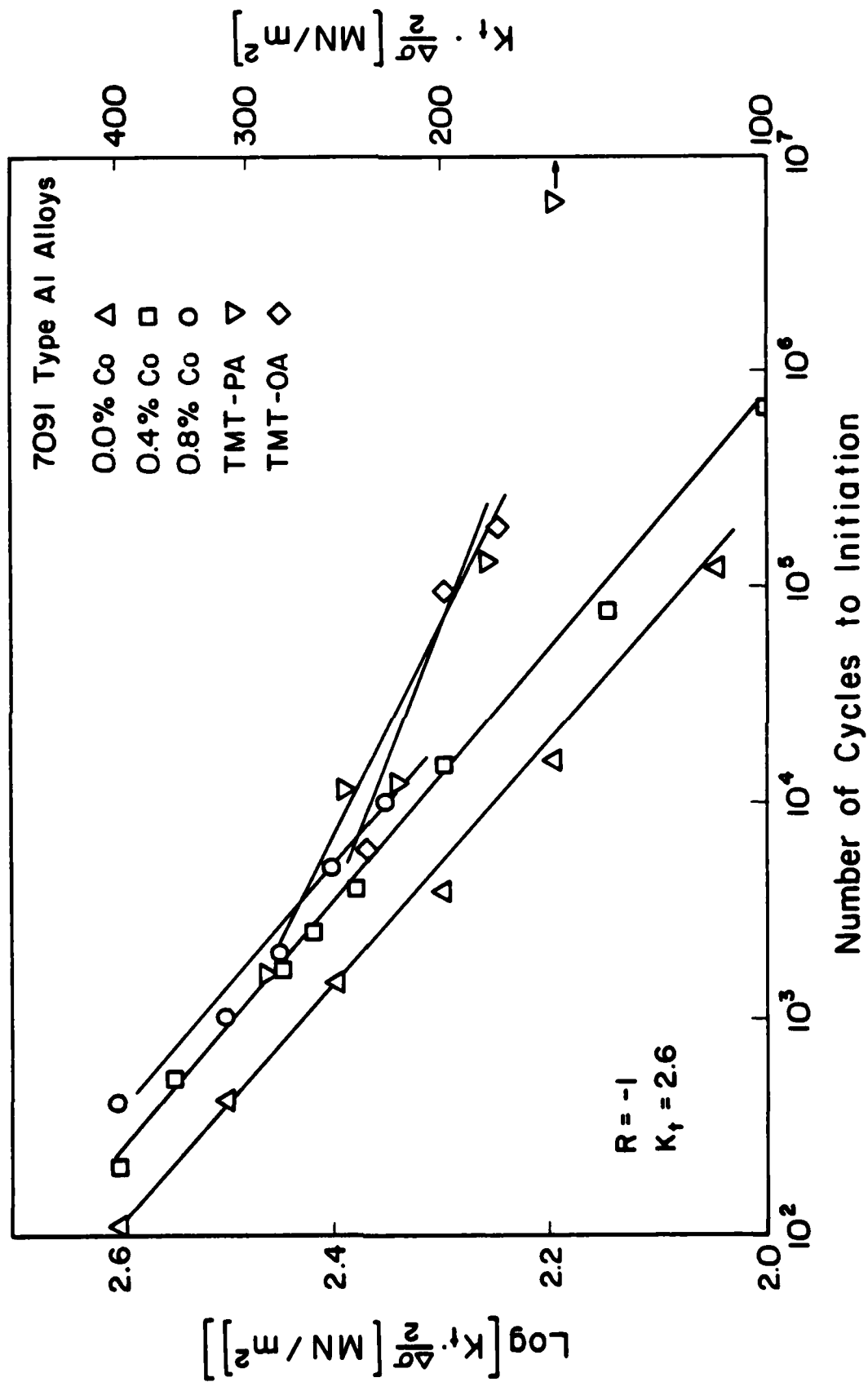


Fig. 17. Number of cycles to initiation of 5 μm cracks versus notch stress in RSP-P/M 0% Co-OA, 7091-OA, and 0.8% Co-OA compared RSP-P/M 0.8% Co-TMT-PA and OA. σ_{max} is the maximum nominal net section stress or the stress amplitude.

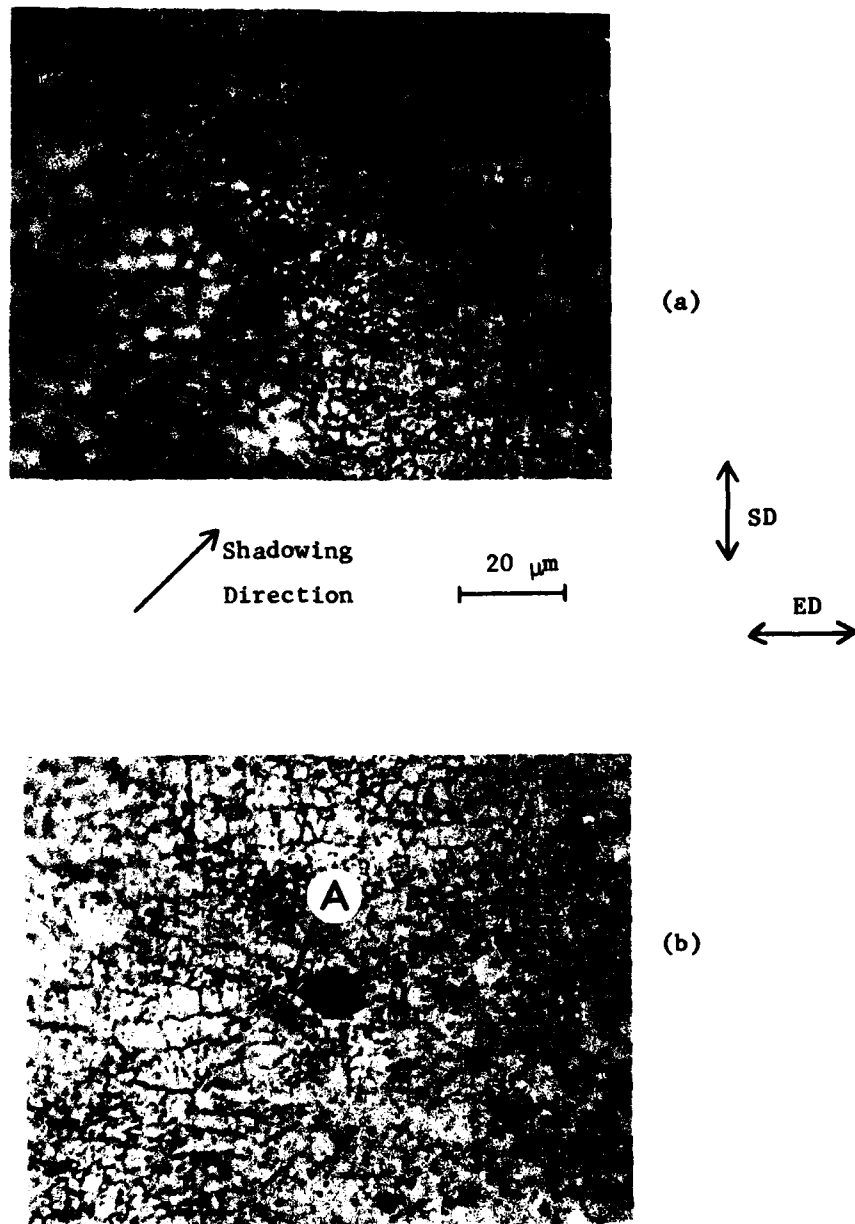


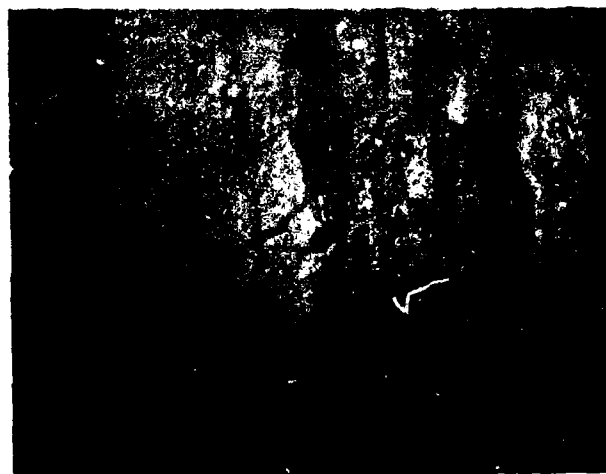
Fig. 18. Optical micrographs of replicas of notch surface of RSP-P/M 7091-OA showing initiation of crack at a defect site. Micrograph (a) is before cycling while (b) is after 23,000 cycles at σ_{\max} (nominal net section) of 126.2 MN/m^2 . The replicas are single stage shadowed with Au-Pd. The notch dimensions were 2 mm depth and 25.4 mm radius of curvature giving K_t of 1.25. The notch orientation was Ln. The arrow indicates the crack.

cycles at a nominal maximum stress of 126 MN/m^2 ($K_t = 1.25$). A small grain boundary crack emanating from the pit is designated by A. The pit no doubt resulted from removal of an inclusion during preparation of the notch. A similar pit and associated crack in a peak aged TMT 0.8% Co sample is shown in Fig. 19a and b. In this experiment the nominal maximum stress was 126 MN/m^2 ($K_t = 1.25$). Figure 19a is after 5020 cycles while Fig. 19b is after 55,000 cycles. Two transgranular cracks are present, a "large" one marked A and a smaller one parallel to the slip markings marked B. Both emanate from the defect. Not all such defects, of course, initiate cracks.

II. Microcrack growth in RSP-P/M X7091 type alloys

Once a fatigue crack forms it spreads sideways on the specimen surface, as well as inward and links up with other cracks that have formed on the specimen surface. On notched specimens the stress concentration factor due to the notch decreases with distance from the notch and this affects the kinetics; however, sideways spreading of microcracks is not affected. Therefore, microcrack growth rates were studied across the length of the notch. The quantity N_{if} was defined following Kung⁴ as the number of cycles until the longest fatigue crack had spread in the notch across the full-thickness of the specimen, in this research 3.5 mm. The difference $N_{if} - N_{ii}$ was taken as the microcrack growth stage.

Figure 20 shows both N_{ii} and N_{if} versus stress for the alloys and treatments studied as well as 2024-T4. Microcrack propagation is obviously much slower in the RSP-P/M X7091 type alloys which have been only extruded and heat treated than in 2024-T4. At all stress levels studied ($N_{if} - N_{ii}$) is much larger for the former. The largest values of N_{if} as well as N_{ii} for a given stress are for the 0.8% Co alloy. From the fatigue point of



(a)

20 μm

SD and
ED



(b)

20 μm

Fig. 19. Optical micrographs of replicas of notch surface of RSP-P/M 0.8% Co-TMT-PA showing initiation of a fatigue crack at a defect. Micrograph (a) is after 2500 cycles at σ_{max} of 125.6 MN/m^2 ($K_t = 1.25$). No crack is seen. After 62,500 (b) two transgranular cracks are seen marked A and B. The B crack is clearly along a slip line.

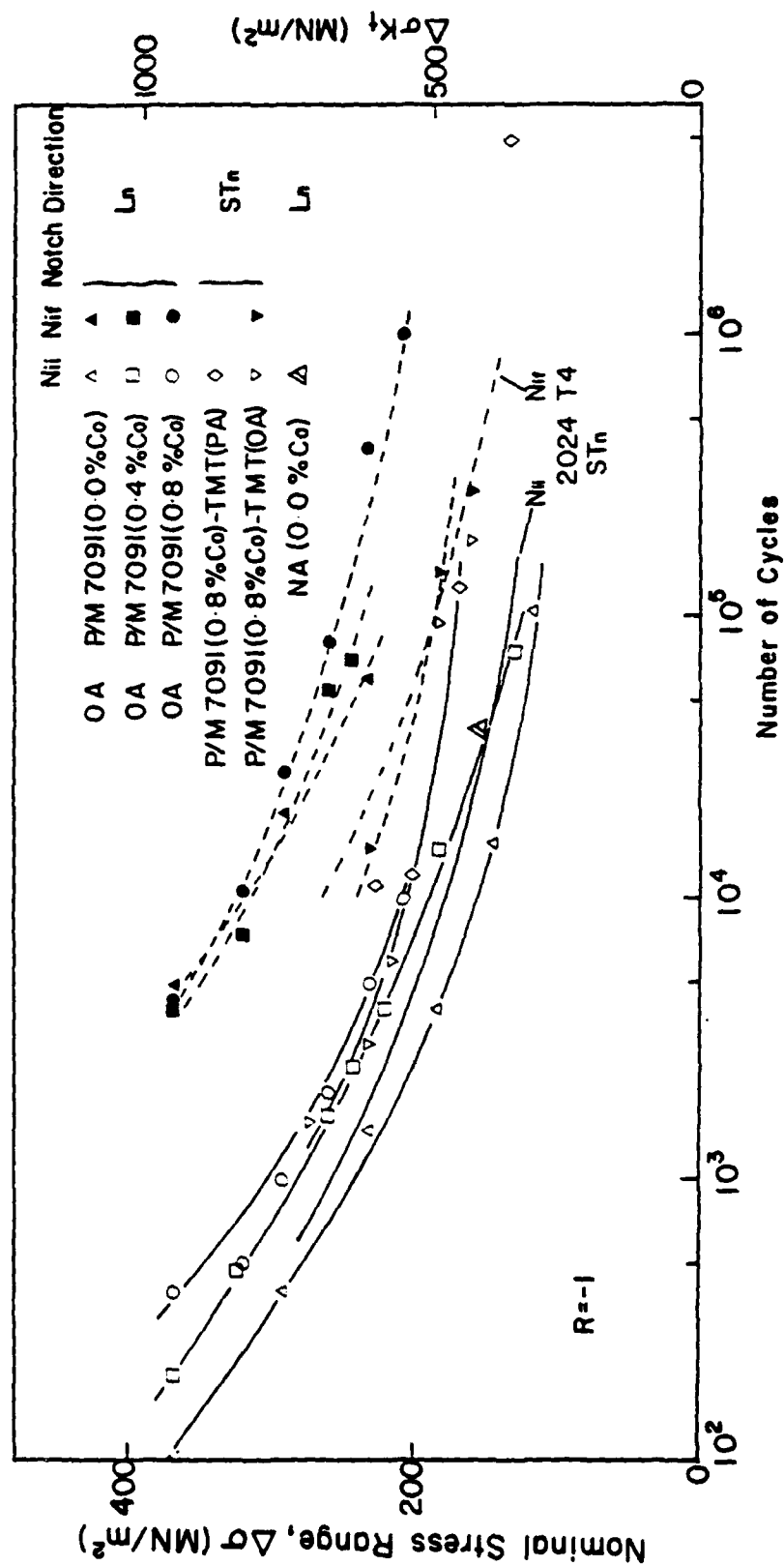


Fig. 20. Number of cycles to initiation, N_{ii} , and number of cycles to 3.5 mm long crack in notch bottom stress, N_{if} . This is same data for N_{ii} as in Figs. 6 and 17. The left hand ordinate is the nominal net section stress range, $\Delta\sigma$, while the right hand ordinate is $K_t\Delta\sigma$.

view, the main virtue of the RSP-P/M X7091 type alloys are their remarkably slow fatigue microcrack growth rates.

The fatigue microcrack propagation rates in the coarse grained thermomechanically treated RSP-P/M 0.8% Co overaged samples are much faster than in the fine grained extruded and heat treated RSP-P/M 0.8% Co alloy. Note that the N_{if} curve is relatively close to the N_{ii} curve for the former.

Some pertinent data from Fig. 20 illustrating the remarkable microcrack propagation resistance of the fine grained RSP-P/M X7091 type alloys are summarized in Table III.

First of all, it should be noted that the stress ranges investigated for the thermomechanically processed 0.8% Co alloy extend to much lower values because their N_{if} values are so small. Comparing TMT against non-TMT samples at 232 MN/m² stress range, N_{if} for the latter is more than 25 times larger. In the high cycle regime N_{ii}/N_{if} is only 1% for as-extruded and overaged samples while after TMT this ratio is $\frac{2}{3}$. Thus while initiation is only a small fraction of the lifetime before TMT, it is a large fraction after TMT. Some data for 2024-T4 are also given. At both 232 and 208 MN/m² strain ranges the N_{if} values are 18 times larger for RSP-P/M 0.8% Co-OA than for 2024-T4.

The microcrack propagation rates are further illustrated in Fig. 21 where the number of cycles are plotted versus the length of the longest crack in the notch. The slower rate for the extruded and overaged condition is immediately obvious. Note the data for this condition was taken at a higher maximum nominal stress (σ_{max}) than for the other two conditions plotted where the microcrack propagation rates are much higher.

Both the TMT treated and room temperature aged samples are quite coarse

TABLE III.

MICROGRAPH PROPAGATION IN RSP-P/M 0.8% Co ALLOY AND 2024-T4

$\Delta\sigma(\text{MN}/\text{m}^2)$	$N_{ii}(\text{cycles})$	$N_{if}(\text{cycles})$	$N_{ii} - N_{if}$	N_{ii}/N_{if}
As extruded, solution treated and overaged				
292	1,000	28,000	27,000	0.04
260	2,000	80,000	78,000	0.03
232	5,000	400,000	395,000	0.01
208	10,000	1,000,000	990,000	0.01
Thermomechanically treated, solution treated and overaged				
232	3,000	15,000	12,000	0.2
180	50,000	150,000	100,000	0.33
164	190,000	290,000	100,000	0.66
2024-T4				
232	2,000	22,000	20,000	0.09
208	4,000	54,000	50,000	0.08

 $K_t = 2.64$ notch

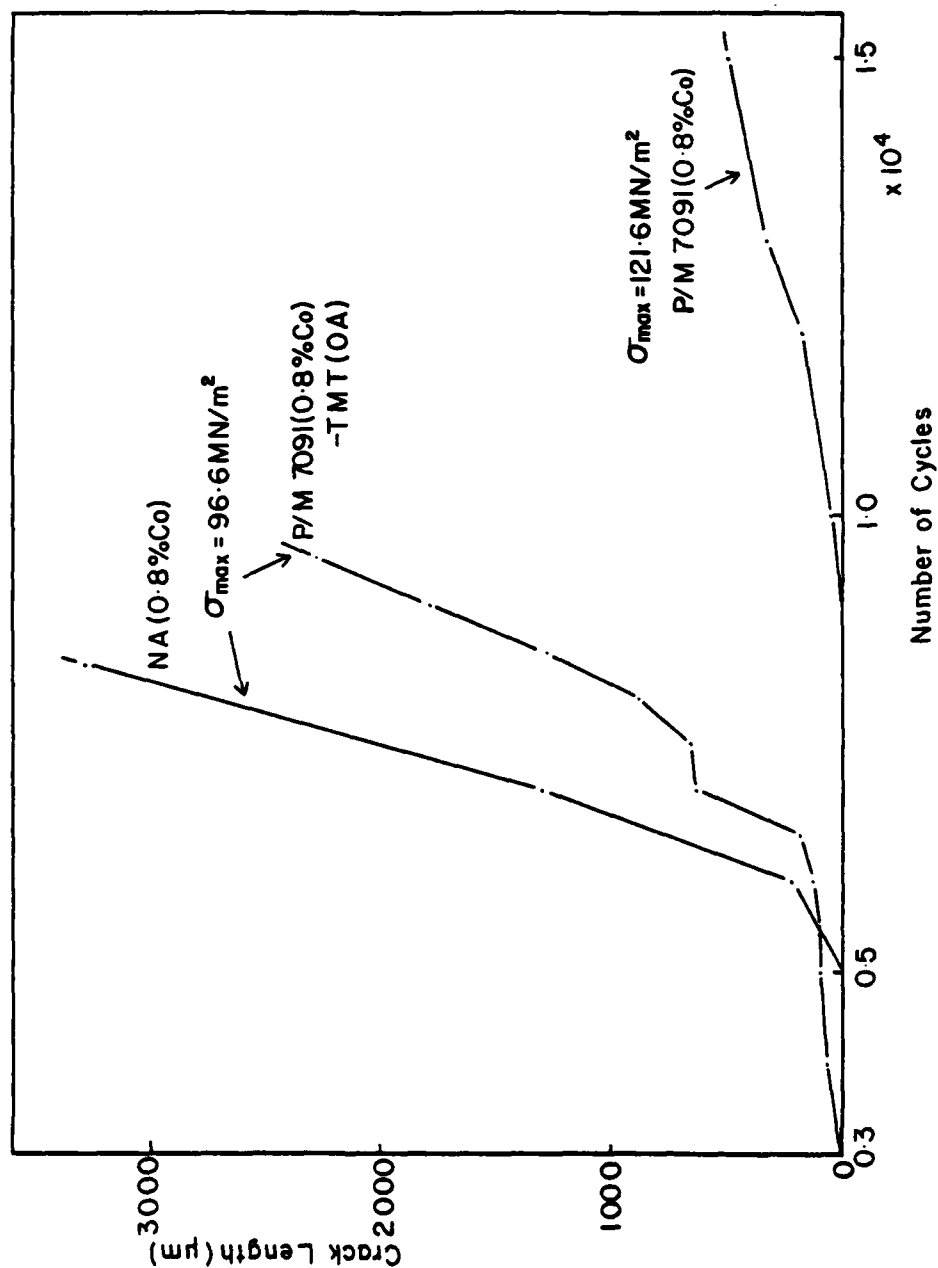


Fig. 21. Length of longest microcrack on the notch surface ($K_t = 2.64$) for RSP-P/M 0.8% Co-OA, RSP-P/M 0.8% Co-NA, and RSP-P/M 0.8%-TMT-OA samples versus number of cycles at the maximum nominal net section stresses indicated.

grained, as already discussed, and the microcrack propagation modes are either fully or mostly transgranular. It is mostly intergranular for the extruded and overaged. The latter is shown in Fig. 9 and was confirmed by many observations in this study. Figure 22a shows a fatigue microcrack in a RSP-P/M 0.8% Co-TMT-PA sample with a $K_t = 1.25$ notch cycled 77,500 times at a maximum nominal net section stress of 126 MN/m^2 . The optical micrograph is of a single stage Au-Pd shadowed replica of the fracture surface. The microcrack which originated at the small defect slightly below the center of the micrograph is clearly along a slip plane for most of its length. A parallel branch crack is in the circle. While a portion of the crack intersection with the notch surface is normal to the stress direction, none of it is intergranular. The microcrack fracture path in the as-extruded and room temperature aged samples was mixed being intergranular and transgranular, as shown in Fig. 23a, which is an optical micrograph of the specimen surface at zero stress. In this experiment σ_{\max} was 141 MN/m^2 and the specimen was cycled 6000 times. The region marked A is transgranular with faint parallel slip lines present. The crack which appears discontinuous under zero stress is clearly continuous (Fig. 23b) under the maximum applied stress.

The very fine grained RSP-P/M X7091 type alloys have a remarkable resistance to growth of microcracks under fatigue loading. The cracks which are mainly along grain boundaries must change direction at grain corners. It is proposed that this tends to blunt the microcracks and slow their growth down. Transgranular cracks are impeded by grain boundaries as evidenced by the fact that they change direction when they intersect a grain boundary but when the grain size is large as after the present thermomechanical treatment

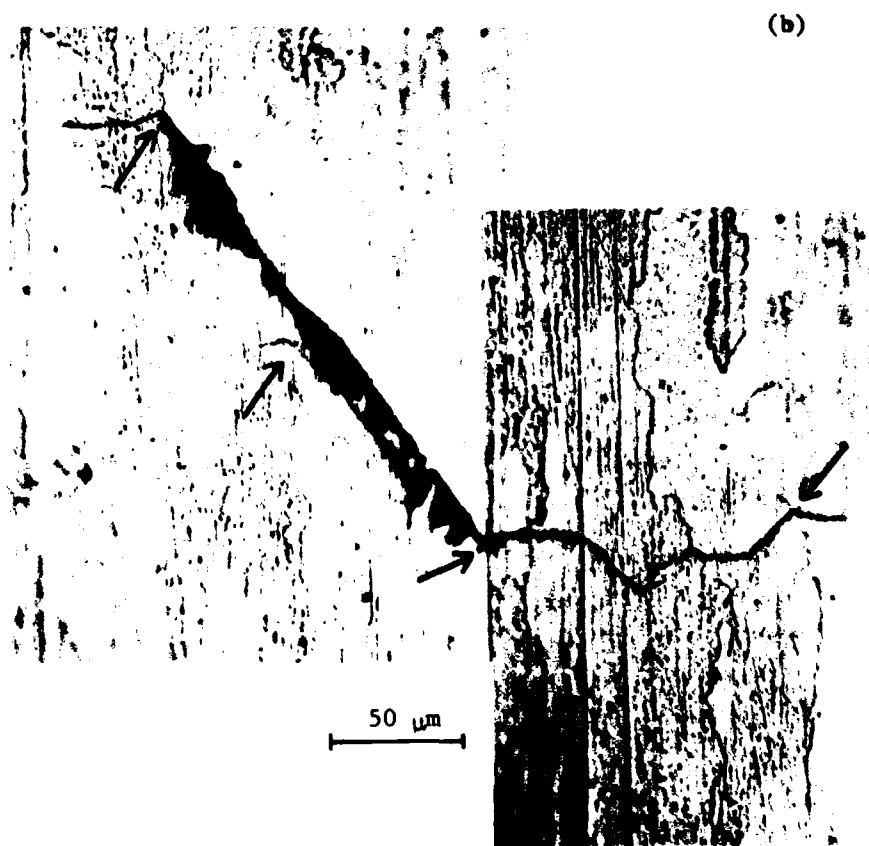
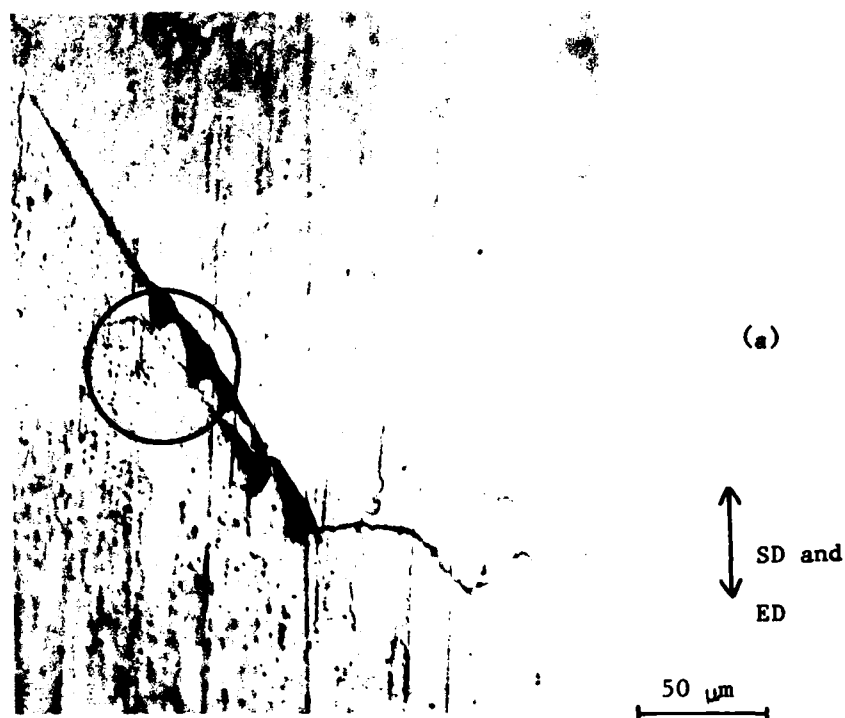
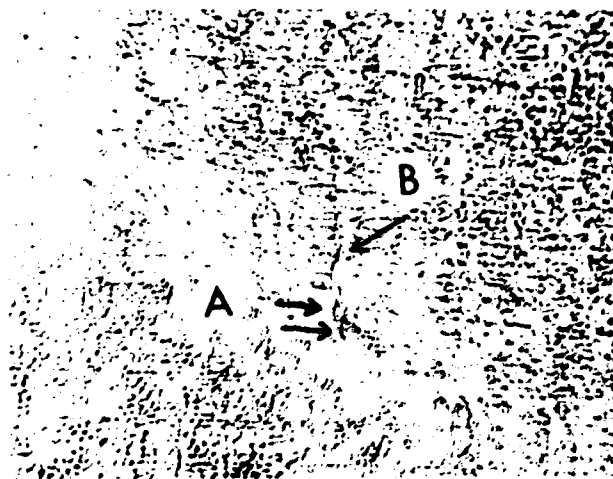


Fig. 22. Optical micrographs of single stage replicas of notch surface ($K_t = 1.25$) for microcrack in RSP-P/M 0.8% Co-TMT-PA cycled at σ_{\max} of $125.6 \text{ MN}/\text{m}^2$ ($R = -1$) for (a) 77,500 cycles and (b) 82,500 cycles. A parallel slip line crack is shown in the circled area. Note the microcrack changes direction at grain boundaries.



(a)

50 μm



(b)

SD
ED

20 μm

Fig. 23. Microcrack in RSP-P/M 0.8% Co-OA sample cycled 6000 times at σ_{\max} of 140.6 MN/m^2 ($R = -1$, $K_t = 1.25$, L_n orientation) (a) optical micrograph of specimen surface at zero stress, (b) optical micrograph of single stage replica with a tensile applied stress to open crack. A shows crack with parallel slip lines. This is transgranular crack. B shows the normal intergranular microcrack.

and the cracks inside the grains are large, the stress intensity at the tip of the crack is sufficiently large to break through the grain boundary to the next grain. It would seem to be very important to test micrograph growth in samples where the TMT was selected to give small grain size and, hopefully, grain boundaries free of oxide segregation. Great resistance to both fatigue crack initiation and microcrack growth is expected.

The resolution treated and room temperature aged samples (designated NA) were also coarse grained, although they contained subgrains. The long grain boundary crack segments initiated evidently also change directions easily at grain corners or generate slip band cracks in neighboring grains.

For macrocrack growth in fine grained RSP-P/M X7091 type alloys, at low ΔK cleavage-like facets are observed while striations are seen at intermediate ΔK s.⁶ The fracture path is transgranular. Thus the intergranular initiation and microcrack growth mode must change to transgranular at some crack size. The fracture surface near the notch surface shows a transition, as shown in Fig. 24, from intergranular to cleavage like. The transition may also be seen in Fig. 9. The transition occurred further from the notch surface as the stress range decreased being 136 μm for σ_{max} of 122 MN/m² and 20 μm for 193 MN/m². The necessity for the transition may also slow down microcrack growth.

III. Near threshold growth of fatigue macrocracks in RSP-P/M X7091 type alloys

Since the near threshold stress intensity range growth rate of materials are very much affected by microstructure and the near threshold or low ΔK growth of fatigue cracks is the most important stage for the design engineer, it was decided to investigate the threshold stress intensity, ΔK_{th} , and the

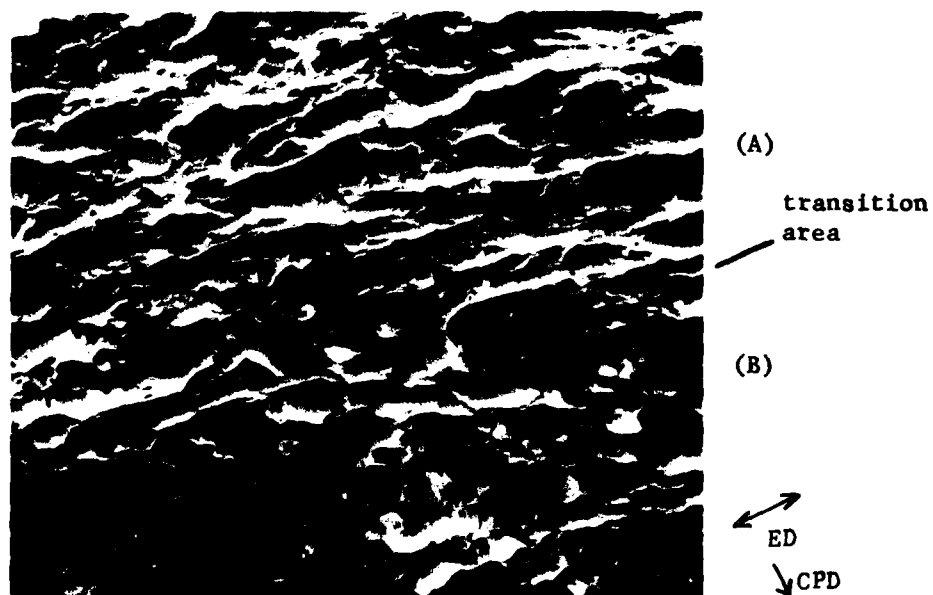


Fig. 24. SEM micrograph of the transition area between the intergranular and the transgranular fracture surface of RSP-P/M 0.8% Co-OA sample. After fatiguing 15,000 cycles at a nominal maximum stress of 61 MN/m^2 the specimen was broken statically. Notch direction was Ln. K_t of this notch was 2.64. 1,000 magnification. CPD: Crack Propagation Direction, ED: Extrusion Direction. $R = 0.1$.
 A: Intergranular fracture surface; B Transgranular fracture surface

near threshold growth rates. Since there is little data on ΔK_{th} for aluminum alloys, it was also necessary to measure some conventional alloys for purposes of comparison.

The measurements were made by the load shedding technique at $R(\sigma_{min}/\sigma_{max}) = 0.05$ using center notched panel specimens $100 \times 32 \times 3.2$ mm. The specimens were lapped with $1 \mu\text{m}$ diamond paste to give a finish suitable for visual observation of the crack lengths using a 40 times magnification telemicroscope attached directly to the electrohydraulic fatigue machine. The center notch was introduced by electrospark machining prior to aging. In reducing the load to approach ΔK_{th} it is very important to do so very gradually. The load shedding was accomplished with decrements less than 8% of the previous load and the crack propagation was measured after the crack had extended several times past the previous plastic zone size. The procedure was repeated until no crack extension was observed during 3×10^6 cycles of loading.

A. RSP-7091 type alloys

Data for RSP-P/M 7091-0A is shown in Fig. 25. The threshold stress intensity range ΔK_{th} was taken to be $0.9 \text{ MN/m}^{\frac{3}{2}}$. This is one-half the value for 2024-T4, as shown in Table IV, and the crack propagation rate at ΔK of $3 \text{ MN/m}^{\frac{3}{2}}$ is three times faster.

Since ΔK_{th} is known to increase with grain size¹³, thermomechanically treated large grain size alloys were also tested. Besides the thermomechanically treated 0.8% Co received from Alcoa Technical Center (Table I-c), samples of the 0.8% Co alloy were cross cold rolled (CCR) 39%, as detailed in Table IV, to give an average grain size of $200 \times 150 \times 100 \mu\text{m}$. All of the large grained TMT-0.8% Co samples had larger thresholds approaching those of

TABLE IV.
THRESHOLD AND NEAR THRESHOLD FATIGUE CRACK GROWTH RATES
IN P/M 7091 TYPE ALLOYS

Alloy and Treatment	ΔK_{th} $MN/m^{3/2}$	da/dN at $3 MN/m^{3/2}$ m/cycle	Environ.
2024-T4	1.8	3×10^{-9}	Air
RSP-P/M 7091-OA	0.9	10×10^{-9}	Air
RSP-P/M 0.8% Co-TMT-OA	1.4	3×10^{-9}	Air
RSP-P/M 0.8% Co-TMT-OA	1.6	2.5×10^{-9}	Argon
RSP-P/M 0.8% Co-CCR*-OA [‡]	1.4	4×10^{-9}	Argon
RSP-P/M 0.8% Co-CCR*-PA	1.6	7×10^{-9}	Argon
RSP-P/M 7091-CCR*-UA [‡]	1.75	5×10^{-9}	Argon

* Cold cross-rolled 39% with initial and two intermediate anneals
1 hr, 475°C, water quenched

‡ OA and UA have same hardness, 91 RB
Solution treated 2 hrs at 488°C and water quenched
Stretched - 3% while being aged 5 to 7 days at R.T.
Underaged - 12 hrs at 121°C
Peak aged - 24 hrs at 121°C
Overaged - peak aged plus 4 hrs at 163°C

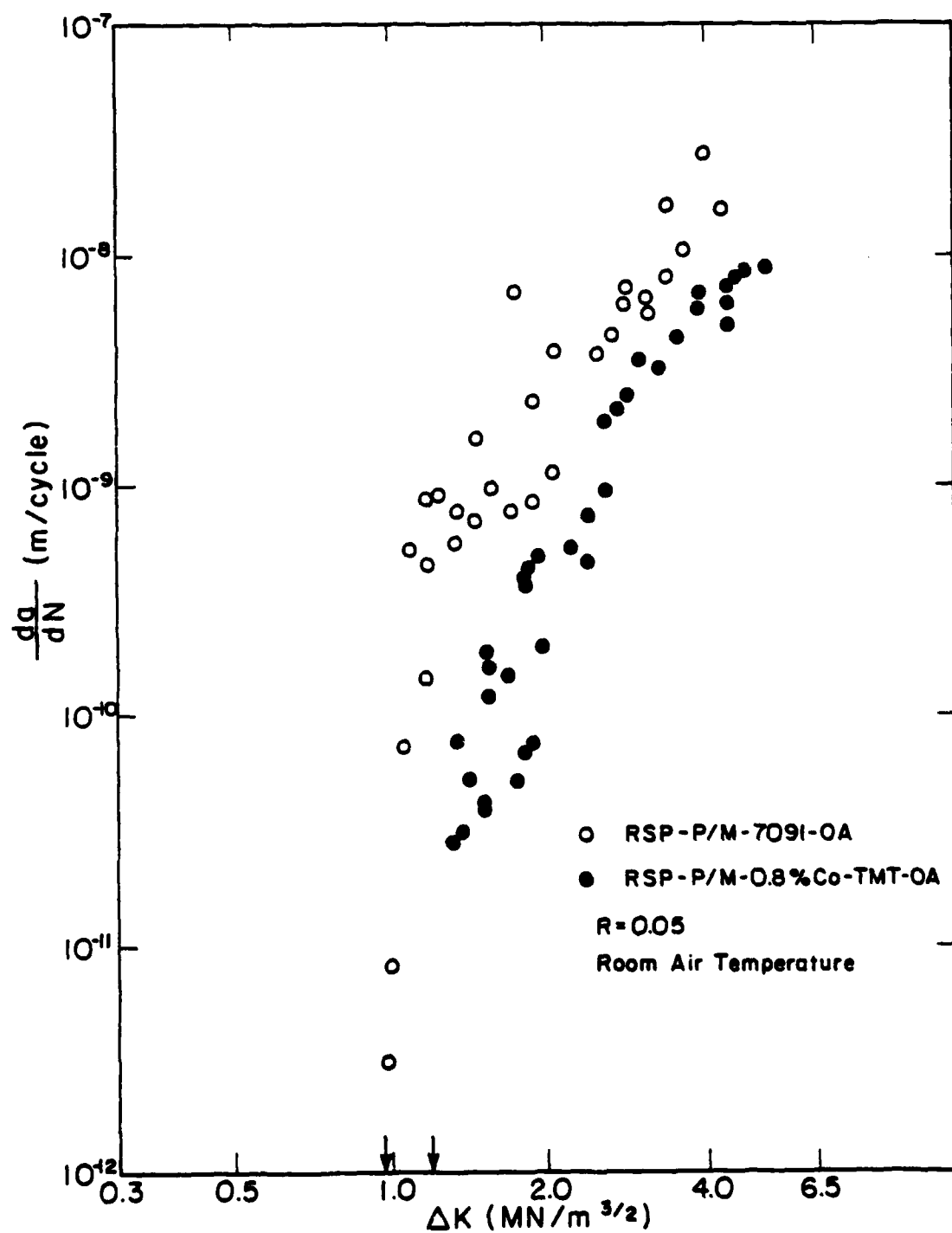


Fig. 25. Near threshold fatigue crack propagation rates (macrocracks) of RSP-P/M 7091-OA and RSP-P/M 0.8% Co-TMT-OA in air at room temperature. $R = 0.05$.

2024-T4, as shown in Table IV and Figs. 25 and 26. The CCR samples were given three aging treatments: underaged, UA; peak aged, PA; and overaged, OA. The aging time at 121°C for the UA samples was selected to give hardness of 91 RB, the hardness of the OA samples. Underaging gave the highest ΔK_{th} but not the lowest value of da/dN at ΔK of $3 \text{ MN/m}^{\frac{3}{2}}$. Of the TMT samples tested, da/dN at ΔK of $3 \text{ MN/m}^{\frac{3}{2}}$ was least for the overaged 0.8% Co-TMT material received from Alcoa. The full da/dN vs. ΔK curves for the CCR samples near threshold are given in Fig. 26.

Thus TMT to give a coarse recrystallized grain size not only increases the resistance to fatigue crack initiation but also increases the threshold stress intensity range for propagation of large cracks. However, microcrack propagation is much faster.

B. Threshold stress intensity range for fatigue crack propagation in 2024-T4 and 2124-T4 aluminum alloys at room temperature and 77° K

The effects of temperature and purity on ΔK_{th} need to be determined and understood in conventional ingot alloys as an aid to designing P/M alloys. Therefore, the stress intensity range, ΔK_{th} , for propagation of large fatigue cracks was measured in ordinary and high purity aluminum alloys, 2024-T4 and 2124-T4 at room temperature and in liquid nitrogen.¹⁴ The results are shown in Table V.

TABLE V.

ΔK_0 FOR 2024-T4 AND 2124-T4 AT 77 AND 300° K

<u>Alloy</u>	<u>Heat Treatment</u>	ΔK_0	
		<u>300° K</u>	<u>77° K</u>
2024	T4	1.8	3
2124	T4	2.1	6
Environment		Air	Liq. N ₂

Units are $\text{MN/m}^{\frac{3}{2}}$, $R = 0.05$

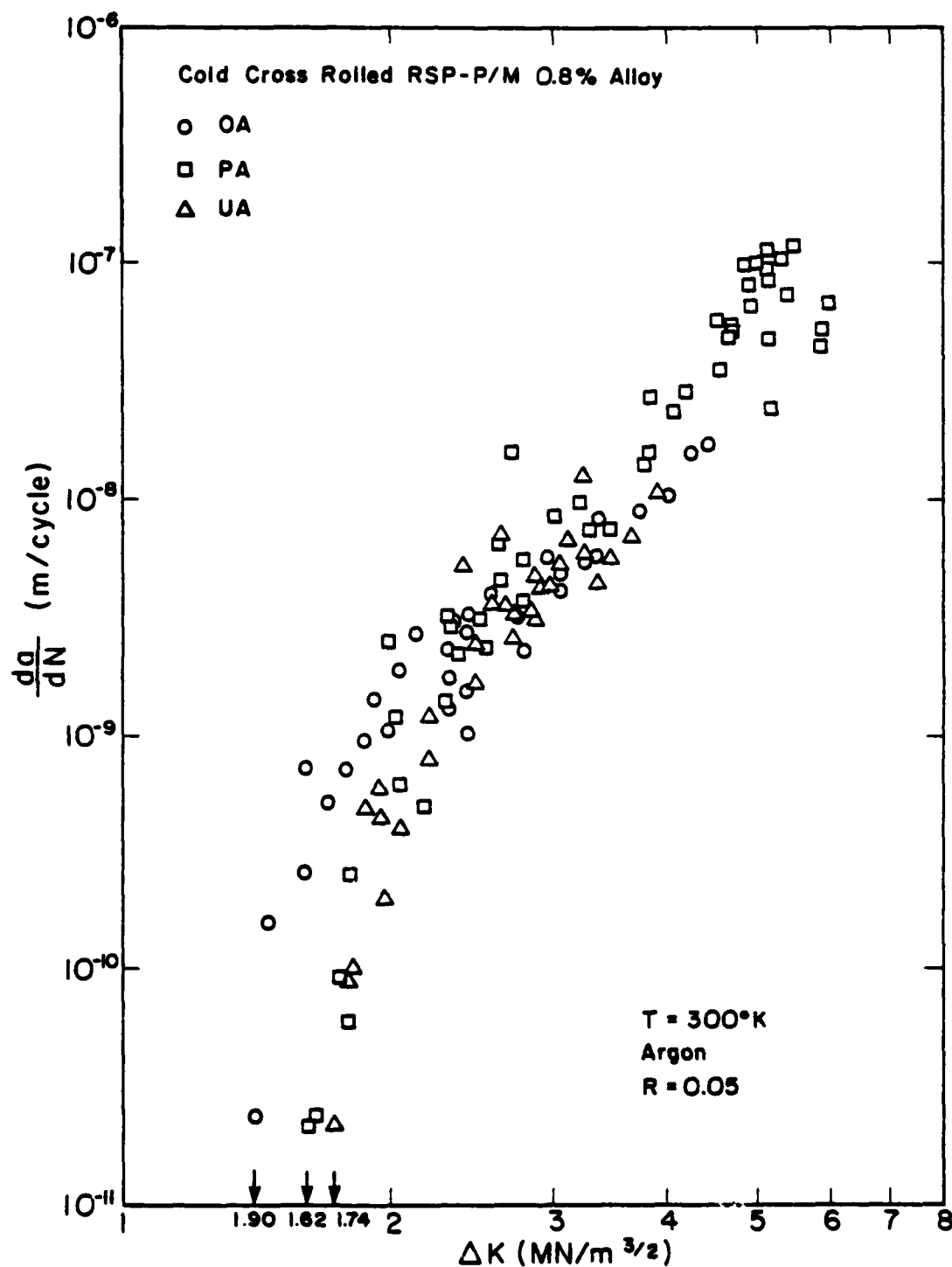


Fig. 26. Near threshold fatigue crack propagation rates of RSP-P/M 0.8% Co alloy cold cross rolled 39%, underaged, peak aged and overaged. See text for heat treatments. Measurements were made in dried argon at room temperature. R = 0.05.

The difference in ΔK_0 between 77 and 300°K is much greater for the high purity alloy, 2124, than for 2024.

Based on the model that the fatigue crack propagation threshold is determined by the stress, σ_s , necessary to operate a dislocation source near the crack tip, Eq.(1) was derived.¹⁵

$$\Delta K_0 \cong \alpha \sigma_s (2\pi s)^{\frac{1}{2}} \quad (1)$$

where s is the distance from the crack tip to the source and α is a factor which takes into account the plastic flow near the crack tip.

Using Eq.(1), the difference between 2024-T4 and 2124-T4 was attributed to a difference in dislocation source, Frank-Read sources for 2024-T4 and double cross-slip for 2124-T4. The constituent particles in 2024 are suggested to be pinning points for sources. The constituent particles are much much further apart in 2124 and, therefore, Frank-Read sources are not thought to be present. Thermal activation is required for double cross-slip but not for F-R sources, explaining the difference in the temperature dependence of ΔK_0 in the two alloys. Using the theory of thermally activated cross-slip for 2124-T4, the computed values of σ_s for 77 and 300°K are somewhat low but reasonable considering the approximations made.

C. Effect of Zr and Cr dispersoids on threshold stress intensity for crack propagation of 7000 type aluminum alloys

Since the effect of dispersoids and constituent particles on threshold should be the same whether the alloys are made by P/M or ingot metallurgy, the threshold stress intensity ranges for propagation of macro-cracks were determined in two high purity 7000 series ingot aluminum alloys obtained from AFML.¹⁵ One had Cr dispersoids ($Al_{12}Mg_2Cr$) which are incoherent

and the other Zr dispersoids (Al_3Zr) which are partially coherent. The compositions are:

TABLE VI.
COMPOSITIONS OF 7XXX ALLOYS

<u>Alloy No.</u>	<u>Cr</u>	<u>Zr</u>	<u>Zn</u>	<u>Mg</u>	<u>Cu</u>	<u>Si</u>	<u>Fe</u>
7475 HP	0.21	-	5.89	2.19	1.50	0.01	0.02
7050 HP	< 0.01	0.12	5.73	2.39	1.50	0.01	0.01
7050 CP	< 0.01	0.12	5.98	2.45	1.52	0.09	0.20

The alloys were studied in the peak aged or T6 heat treated condition. The Zr containing HP alloy was also studied in the overaged condition. Peak strength was achieved by solutionizing for 1 hr at 475°C, water quenching, stretching 3%, aging at room temperature for 5 to 7 days, and then aging for 24 hrs at 121°C. Overaging was the previous plus 24 hrs at 163°C. The samples were water quenched after elevated temperature aging.

The data are summarized in Table VII and the near threshold da/dN data are plotted in Figs. 27 and 28.

TABLE VII.
THRESHOLD STRESS INTENSITY RANGES OF Cr AND Zr
7000 Al ALLOYS

	<u>Heat Treatment</u>	<u>ΔK_0 (MN/m^{3/2})</u>
7475 HP	T6	1. /
7050 HP	T6	2.1
7050 HP	OA	1.7
7050 CP	T6	2.4

Using Zr-dispersoids gives a higher ΔK_0 than Cr-dispersoids. This may result because the Al_3Zr is partially coherent with the matrix while $\text{Al}_{12}\text{Mg}_2\text{Cr}$

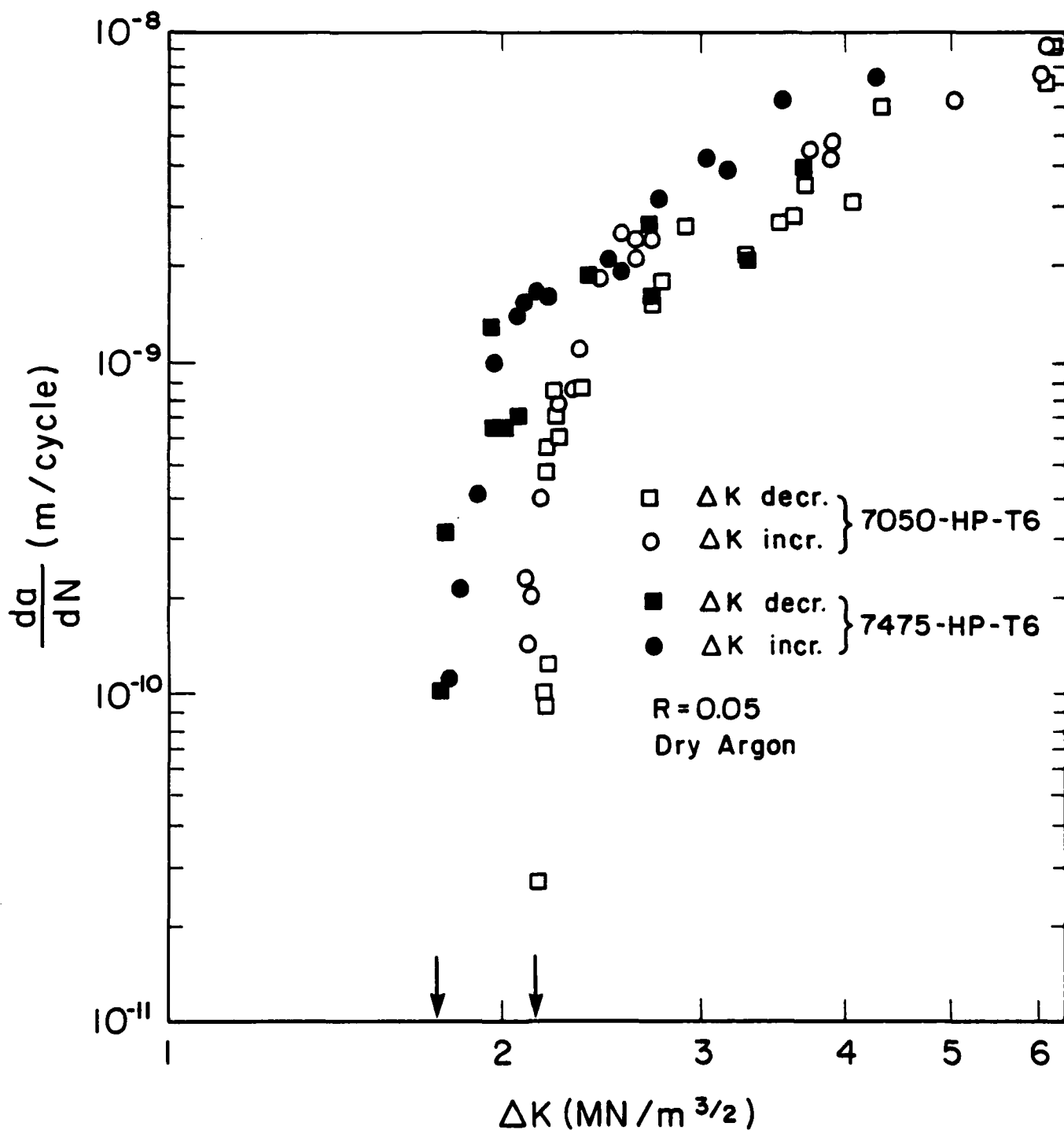


Fig. 27. Comparison of near threshold fatigue crack propagation rates in 7050-HP-T6 and 7475-HP-T6. High purity (HP) 7050 alloy contains Al_3Zr dispersoids while high purity 7475 contains $Al_{12}Mg_2Cr$ dispersoids.

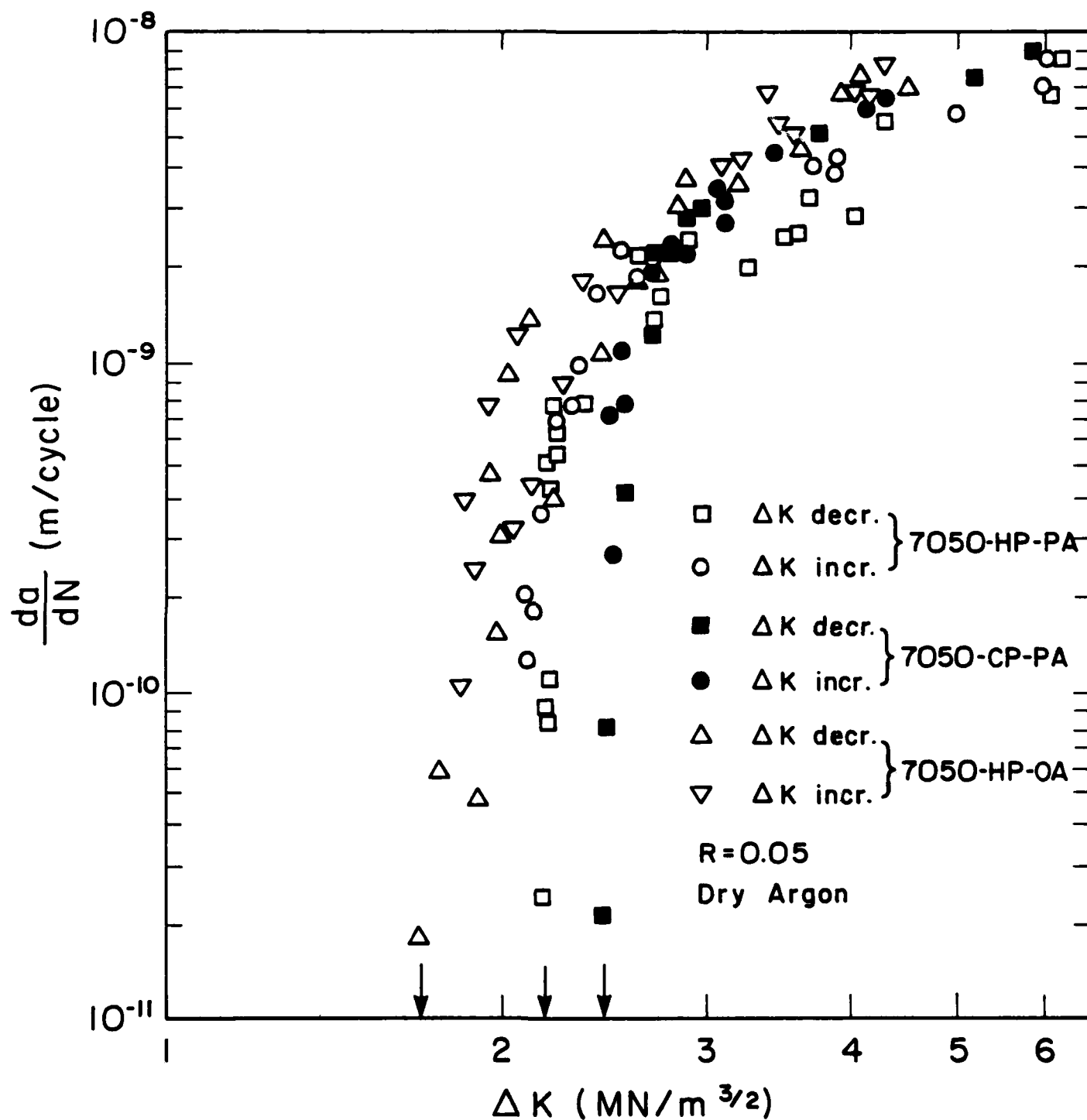


Fig. 28. Comparison of near threshold fatigue crack propagation rates in HP-7050 peak aged (T6) and overaged samples with commercial purity (CP) 7050-T6 samples.

is not. Severe overaging reduces ΔK_{th} . This may be due to a precipitate free zone near grain boundaries, large η particles at grain boundaries, as well as replacement of the coherent η' precipitates inside the grains by η which is incoherent.

The increase in ΔK_{th} from the large constituent particles was unexpected but may result from homogenization of the plastic deformation.¹⁶ With coherent precipitates and dispersoids dislocations cut the particles with little work hardening and the plastic deformation tends to be localized. The presence of some large incoherent particles increases the work hardening rate because the dislocations must bypass them by cross-slip or the Orowan mechanism. While coherent small dispersed phases which are very close together are preferable to incoherent small closely spaced dispersed phases for increasing strength, a few large incoherent particles appear to be beneficial for increasing ΔK_{th} . The larger ΔK_{th} for the commercial purity alloy is an observation of considerable practical importance.

SUMMARY AND CONCLUSIONS

1. In fine grained RSP-P/M 7091 type alloys extruded and age hardened the fatigue cracks initiate along grain boundaries. The resistance to initiation, as measured by the cycles to initiation vs. applied stress amplitude, increases with Co content from 0 to 0.8%. The previously determined data for 2024-T4 falls among the data for the above alloys but for 2024-T4 the fatigue cracks are initiated along slip lines. The expected increase in resistance to initiation of fatigue cracks due to the small grain size and small dispersed particle size in the RSP-P/M was not achieved due to the grain boundary embrittlement.

2. The grain boundary fatigue crack initiation was attributed to the presence of oxide particles at certain grain boundaries. The embrittlement is not due to segregation of incoherent η precipitates to grain boundaries nor to the presence of a precipitate free zone.

3. In coarse grained recrystallized thermomechanically treated 0.8% Co alloy, the grain boundaries were not embrittled and the fatigue cracks initiated along slip bands. Tested in the overaged condition, the TMT samples of this alloy had much greater resistance to fatigue crack initiation than when only heat treated after extrusion. It should be of great interest to investigate fatigue crack initiation in thermomechanically treated RSP-P/M 7091 type alloys where the TMT is selected to give small grain size.

4. Once small fatigue cracks have initiated, the fine-grained RSP-P/M 7091 type extruded and heat treated alloys have a remarkable resistance to growth of microcracks. This growth occurs mainly along grain boundaries and is very slow.

5. In the coarse-grained recrystallized TMT 0.8% Co alloy microcrack growth occurs along slip lines and is very fast. Such microcracks are stopped by grain boundaries; therefore, it should also be of great interest to investigate microcrack growth in TMT samples where the TMT is selected to give small grain size.

6. The threshold stress intensity for propagation of large cracks, ΔK_{th} , in fine grained RSP-P/M 7091-OA (extruded and aged) is very low, about half that for 2024-T4; however, the coarse grained TMT RSP-P/M 7091 type alloys have ΔK_{th} values approaching that of 2024-T4.

7. In ingot metallurgy 7000 series aluminum alloys, Zr dispersoids,

which are semi-coherent, lead to larger ΔK_{th} than Cr dispersoids which are not. Commercial purity 7050 has a larger ΔK_{th} than high purity 7050. The dispersoids are thought to homogenize the plastic deformation.

REFERENCES

1. J. P. Lyle, Jr. and W. S. Cebulak, "Powder Metallurgy Approach for Control of Microstructure and Properties of High Strength Aluminum Alloys", Met. Trans. 6A, 685 (1975).
2. W. L. Otto, Jr., "Metallurgical Factors Controlling Structure in High Strength Aluminum P/M Products", AFML Contract No. F33615-74-C-5077, AFML Report No. TR-76-60, May 1976, Alcoa Technical Center, Alcoa Center, PA.
3. R. E. Sanders, Jr., W. L. Otto, Jr., and R. J. Bucci, "Fatigue Resistant Aluminum P/M Alloy Development", AFML Contract No. F33615-77-C-5174, AFML Report No. TR-79-4131, September 1979, Alcoa Technical Center, Alcoa Center, PA.
4. C. Y. Kung and M. E. Fine, "Fatigue Crack Initiation and Microcrack Growth in 2024-T4 and 2124-T4 Aluminum Alloys", Met. Trans. 10A, 603 (1979).
5. J. P. Lyle, Jr. and W. S. Cebulak, "Properties of High-Strength Aluminum P/M Products", Metals Eng. Quarterly 14, No. 1, 52 (1974).
6. A. Lawley and M. J. Koczak, "A Fundamental Study of Fatigue in Powder Metallurgy Aluminum Alloys", Final Technical Report, AFOSR Grant No. 77-3247, August 1981, Drexel University, Philadelphia, PA.
7. E. A. Starke, Jr., Georgia Institute of Technology, Atlanta, GA. Private communication.
8. R. E. Peterson, "Stress Concentration Design Factors", John Wiley and Sons, New York (1953).
9. H. Neuber, "Theory of Notch Stresses: Principles for Exact Stress Calculations", Lithoprinted by J. W. Edwards, Ann Arbor, MI (1946).
10. J. A. Walker and E. A. Starke, Jr., To be published; J. A. Walker, "Microstructure and Properties of Extruded P/M CT91-T7X151", M.S. Thesis, Georgia Institute of Technology, Atlanta, GA, December 1980.
11. E. A. Starke, Jr. and G. Lütjering, "Cyclic Plastic Deformation and Microstructure" in Fatigue and Microstructure, ed. by M. Meshii, ASM 1979, p. 205.

12. V. Kuo and E. A. Starke, Jr., To be published; V. Kuo, "The Effects of P/M processing and Intermediate Thermal Mechanical Treatment on the Fatigue Properties of High Strength Aluminum Alloys, X7091", M.S. Thesis, Georgia Institute of Technology, Atlanta, GA, August 1981.
13. M. E. Fine and R. O. Ritchie, "Fatigue Crack Initiation and Near-Threshold Crack Growth" in Fatigue and Microstructure, ed. by M. Meshii, ASM, 1979, p. 245.
14. J. McKittrick, P. K. Liaw, S. I. Kwun and M. E. Fine, "Threshold for Fatigue Macrocrack Propagation in Some Aluminum Alloys", Met. Trans. 12A, 1535 (1981).
15. J. S. Santner and D. Eylon, "Fatigue Behavior and Failure Mechanisms of Modified 7075 Aluminum Alloys", Met. Trans. 10A, 841 (1979).
16. M. E. Fine, "Precipitation Hardening of Aluminum Alloys", Met. Trans. 6A, 625 (1975).

LIST OF PUBLICATIONS -- AF SUPPORTED

1. "Fatigue Crack Initiation and Near-Threshold Crack Growth", M. E. Fine and R. O. Ritchie, 1978 ASM Materials Science Seminar: Fatigue and Microstructure, St. Louis, Missouri, Proceedings, M. Meshii, ed., ASM, p. 245 (1979).
2. "Fatigue Crack Initiation and Microcrack Growth in 2024-T4 and 2124-T4 Aluminum Alloys", C. Y. Kung and M. E. Fine, Met. Trans. 10A, 603 (1979).
3. "Role of Plastic Work in Fatigue Crack Propagation in Metals", Y. Izumi and M. E. Fine, Eng. Fract. Mech. 11, 791 (1979).
4. "An Electrohydraulic Fatigue Apparatus for Testing at Cryogenic Temperature", P. K. Liaw and J. Baker, Rev. Sci. Instrum. 50(12) (Dec. 1979).
5. "Fatigue Resistance of Metals", M. E. Fine, ASM Campbell Lecture, Met. Trans. 11A, 365 (1980).
6. "Dependence of Cyclic Plastic Work of Fatigue Crack Propagation on ΔK in MA87 Aluminum P/M Alloy", S. I. Kwun and M. E. Fine, Scripta Met. 14, 155 (1980).
7. "Comparison of Plastic Work of Fatigue Crack Propagation in Low Carbon Steel Measured by Strain-Gages and Electron Channeling", P. K. Liaw, M. E. Fine and D. L. Davidson, Fatigue of Eng. Mater. & Stru. 3, 59 (1980).
8. "Plastic Work of Fatigue Crack Propagation in Steels and Aluminum Alloys", P. K. Liaw, S. I. Kwun and M. E. Fine, Met. Trans. 12A, 49 (1981).
9. "Threshold for Fatigue Macrocrack Propagation in Some Aluminum Alloys", J. McKittrick, P. K. Liaw, S. I. Kwun and M. E. Fine, Met. Trans. 12A, 1535 (1981).
10. "Threshold for Fatigue Failure", M. E. Fine, Bull. JIM 20, No. 8, 668 (1981).
11. "Energy Considerations in Fatigue Crack Propagation", Y. Izumi, M. E. Fine and T. Mura, Int. J. Fract. 17, 15 (1981).
12. "Fatigue Crack Propagation in 99.99⁺ and 1100 Aluminum at 298 and 77 K", P. K. Liaw and M. E. Fine. In press, Metallurgical Transactions A.
13. "Fatigue Crack Initiation and Microcrack Propagation in High Stress Aluminum P/M Alloys", S. Hirose and M. E. Fine. To be published in Conference Proceedings volume of Symposium on Powder Metallurgy of Aluminum Alloys to be held at AIME Annual Meeting, Dallas Texas, February 1982.
14. "Near Threshold Fatigue Crack Propagation in High Stress Aluminum P/M Alloys", L. C. Filler, M. Zedalis and M. E. Fine. In preparation.

PAPERS AND TALKS PRESENTED -- AF SUPPORTED

1. 1978 ASM Materials Science Seminar: Fatigue and Microstructure, "Fatigue Crack Initiation and Near-Threshold Crack Growth", M. E. Fine and R. O. Ritchie, October 1978, St. Louis, Missouri.
2. 1979 AIME Annual Meeting, "Fatigue Properties of 99.99⁺ and 1100 Al at 298° K and 77° K in Some Aluminum Alloys", J. M. McKittrick, P. K. Liaw and M. E. Fine, September 1979, Milwaukee, Wisconsin.
3. 1979 ASM Annual Meeting, Campbell Lecture, M. E. Fine, "Fatigue Resistance of Metals", November 14, 1979, Chicago, Illinois.
4. 1979 Japan Institute of Metals Fall Meeting, "Thresholds for Fatigue Failure" (invited paper), October 16, 1979, Nagoya, Japan.
5. 1980 AIME Annual Meeting, "Comparison of Plastic Work of Fatigue Crack Propagation in Low Carbon Steel Measured by Strain Gages and Electron Channeling", P. K. Liaw, M. E. Fine and D. L. Davidson, February 26, 1980, Las Vegas, Nevada.
6. 1980 AIME Annual Meeting, "Plastic Work of Fatigue Crack Propagation in Steels and Aluminum Alloys", P. K. Liaw, S. I. Kwun and M. E. Fine, February 26, 1980, Las Vegas, Nevada.
7. 1980 TMS-AIME Fall Meeting, "Fatigue Properties in Aluminum at 298 and 77° K", P. K. Liaw and M. E. Fine, October 6, 1980, Pittsburgh, Pa.
8. 1980 TMS-AIME Fall Meeting, "Fatigue Crack Initiation and Microcrack Growth in Precipitation Hardened Powder Metallurgy Aluminum Alloys", S. Hirose and M. E. Fine, October 6, 1980, Pittsburgh, Pa.
9. Metallurgy colloquium talk, University of Illinois, "Thresholds for Fatigue Crack Initiation, Microcrack Propagation and Macrocrack Propagation", April 10, 1980, Urbana, Illinois.
10. Cullity Memorial Lecture, Notre Dame University, "Metallurgical Factors Affecting Fatigue", March 4, 1981, South Bend, Indiana.
11. Colloquium talk, Purdue University, "Metallurgical Factors Affecting Fatigue", April 20, 1981, West Lafayette, Indiana.
12. ASM Chicago Chapter meeting, "Fatigue of Metals", April 13, 1981, Chicago, Illinois.
13. Golden Gate Metals and Welding Conference, "Measurement and Theory of Elastic Constants in Solids", January 20-23, 1981, San Francisco, CA.
14. Proceedings, Review of Government Sponsored Work in Structural Aluminum Powder Metallurgy, "Fatigue Crack Initiation and Propagation in MA87 and Related Alloys" M. E. Fine and Group at Northwestern University, February 12-13, 1980, Dayton, Ohio.

LIST OF PROFESSIONAL PERSONNEL WHO PARTICIPATED IN THE RESEARCHPrincipal Investigator

Morris E. Fine, Walter P. Murphy Professor of Materials Science and Engineering

Postdoctoral Research Associates

S. I. Kwun, 6/15/78 - 9/30/79 ($\frac{1}{2}$ time)
S. Tsunekawa, 1/6/81 - 12/15/81 ($\frac{1}{2}$ time)

Graduate Students

J. McKittrick - Completed M.S. August 1979. Now at International Harvester Company, Science & Technology, Hinsdale, Illinois.
P. K. Liaw - Completed Ph.D. June 1980. Now at Westinghouse Research and Development Center, Pittsburgh, Pennsylvania.
L. C. Filler - Completed M.S. June 1981. Now at Texaco, Beaumont, Texas.
S. Hirose - Completed Ph.D. August 1981. Now at Ryobi, Ltd., Fuchu, Hiroshima, Japan.
M. Zedalis, Ph.D. student - Research topic: near threshold fatigue crack propagation in ingot and powder metallurgy aluminum alloys.

Secretary

J. Bell ($\frac{1}{2}$ time)

DISSERTATIONS

1. "Near-Threshold Fatigue Crack Propagation in Several Al Alloys at 300°K and 77°K", J. McKittrick, M.S. awarded August 1979.
2. "Fundamental Studies of Fatigue Crack Propagation in Metals", P. K. Liaw, Ph.D. awarded June 1980.
3. "Effect of Dispersoid, Purity and Overaging on Threshold for Macro-fatigue Crack Propagation in Al-Zn-Mg-Cu Alloys", M.S. awarded June 1981.
4. "Fatigue Crack Initiation and Microcrack Growth in Precipitation Hardened P/M Aluminum Alloys", S. Hirose, Ph.D. awarded August 1981.
5. "Near Threshold Fatigue Crack Propagation and Microstructure in Some I/M and P/M Aluminum Alloys", M. Zedalis, M.S. to be awarded January 1982.

DATA
FILM

2-